

**ENHANCED ANIMAL CLONING: THE EFFECTS OF  
DEMECOLCINE ON THE ANAPHASE PROMOTING COMPLEX  
IN MAMMALIAN OOCYTE DEVELOPMENT**

A THESIS

Submitted to the Faculty

of the

WORCESTER POLYTECHNIC INSTITUTE

In partial fulfillment of the requirements for the

Degree of Master of Science

in

Biology and Biotechnology

by

---

Paul Troccolo

December 15, 2008

APPROVED:

---

Eric W. Overstrom, Ph. D.  
Major Advisor

---

David Adams, Ph. D.  
Committee Member

---

Samuel Politz, Ph. D.  
Committee Member

## Abstract

The efficiency of somatic cell nuclear transfer has been improved slightly with the use of Demecolcine as a chemical enucleant. While the reasons for this improved efficiency remain unclear, it has been hypothesized that the Demecolcine assisted enucleation procedure is less exigent to vital cell processes within the oocyte including the Anaphase-Promoting Complex (APC) dependent ubiquitination of proteins. In order to test the effect of Demecolcine on the APC, the spatial localizations of Apc11, the catalytic core of the complex, and Cdc20, a main activator of the complex, were studied in developing mouse oocytes. In control oocytes, a high concentration of Apc11 protein was observed surrounding the meiotic spindle, but this perispindular localization was not observed in oocytes treated with Demecolcine. Similarly, oocytes stained for Cdc20 also demonstrated cytoplasmic localization in control oocytes with a variation consistent with previous studies in total protein at different stages of development. However, in oocytes treated with Demecolcine, this developmental variation was not observed. These data suggest that since both Apc11 and Cdc20 localization are affected by an incubation in Demecolcine, the activity of the APC would also be affected. In order to test this theory, Rec8, a meiotic specific member of the cohesion complex, was localized in developing mouse embryos. Since the destruction of Rec8 is a downstream consequence of the ubiquitination pathway, Rec8 localization serves as an indirect indicator of APC activity. The data indicate Rec8 localization was only subtly influenced by Demecolcine, thus the magnitude of the drug's effect APC activity remains unclear. (249words)

## Table of Contents

Abstract.....	2
Table of Contents.....	3
Table of Figures.....	5
Introduction.....	6
Literature Review.....	8
Animal Cloning Techniques.....	8
Creation of a Cytoplasm.....	8
Embryo Reconstruction.....	9
Activation and Development.....	10
Anaphase Promoting Complex Background.....	12
APC in somatic cells.....	12
APC in M2 eggs.....	14
APC Subunits.....	16
Apc11/Apc2 as the catalytic core.....	16
Structure of Apc11 RING finger.....	16
Structure of Apc2.....	17
Apc10 (Doc1).....	17
Apc1 (Tsg24).....	18
Tetratricopeptide TPR repeats (Apc3, Apc6, Apc7, Apc8).....	18
Apc4, Apc5.....	19
Apc9, Cdc26.....	19
Apc13(Swm1), Apc14, Apc14(Mnd2).....	19
Cdc20 (Fizzy).....	19
APC localization and activity.....	20
Cytoskeleton Affecters.....	21
Intermediate Filaments.....	21
Microfilaments.....	21
Microtubules.....	24
Materials and Methods.....	28
Oocyte collection.....	28
Oocyte activation.....	28
Oocyte fixation.....	29
Oocyte staining and imaging.....	29
Antibody optimization.....	31
Hela cell culture.....	31
Concentration study.....	31
Results.....	33
Part I: Antibody validation.....	33
Part II: Optimization.....	36
Dilution study.....	36
Incubation temperature and duration.....	40
Fixative comparison.....	41
Selection of an activation stimulus.....	42

Part III. Apc11 Localization .....	42
Control activation.....	44
Effects of Demecolcine on Apc11 spatial localization.....	46
Part IV. Cdc20 Localization .....	50
Control activation.....	50
Effects of Demecolcine on Cdc20 localization.....	52
Part V: Rec8 Localization.....	55
Control activation experiments .....	55
The effects of Demecolcine on Rec8 localization .....	59
Discussion.....	61
The effects of Demecolcine on the APC.....	61
Implications for SCNT.....	63
Future Experiments.....	64
Works Cited .....	66
Appendix A: Hela cell split protocol .....	72
Appendix B: Chemical Components .....	72
Media Composition.....	72
FHM.....	72
KSOM.....	74
MTSB-XF .....	75
Blocking Buffer .....	75
Blocking Buffer (-goat serum).....	76

## Table of Figures

Figure 1 - Initiation of Anaphase by the APC (Peters, 2002).....	13
Figure 2 - APC activity (Zacharaie <i>et al.</i> , 1999).....	14
Figure 3 - Negative control images of Hela cells .....	33
Figure 4 - Localization of APC subunits in unsynchronized HeLa cells.....	34
Figure 5 - Published images of APC3 localization (Acquaviva <i>et al.</i> 2004).....	35
Figure 6 - Localization of Rec8 in unsynchronized HeLa cells.....	36
Figure 7 - Negative control images of oocytes .....	38
Figure 8 - Apc11 staining optimization in mouse oocytes. ....	39
Figure 9 - Examples of Cdc20 optimization .....	40
Figure 10 - Oocytes fixed with MTSB-XF. ....	41
Figure 11 - Localization of Apc11 in oocytes arrested at Metaphase of meiosis II (MII). .....	44
Figure 12 - Localization of Apc11 in oocytes fixed at Anaphase of meiosis II (AII). ....	45
Figure 13 - Localization of Apc11 in oocytes fixed at Telophase of meiosis II (TII). ....	45
Figure 14 - Localization of Apc11 in oocytes fixed in Interphase. ....	46
Figure 15 - Effects of Demecolcine on Apc11 localization in oocytes fixed at AII. ....	47
Figure 16 - Effects of Demecolcine on Apc11 localization in oocytes fixed at TII. ....	48
Figure 17 - Effects of Demecolcine on Apc11 localization in oocytes fixed at Interphase. .....	49
Figure 18 - Localization of Cdc20 in oocytes fixed at MII. ....	50
Figure 19 - Localization of Cdc20 in oocytes fixed at AII. ....	51
Figure 20 - Localization of Cdc20 in oocytes fixed at TII. ....	52
Figure 21 - Localization of Cdc20 in oocytes fixed at Interphase. ....	52
Figure 22 - Effects of Demecolcine on Cdc20 localization in oocytes fixed at AII. ....	53
Figure 23 - Effects of Demecolcine on Cdc20 localization in oocytes fixed at TII. ....	54
Figure 24 - Effects of Demecolcine on Cdc20 localization in oocytes fixed at Interphase. .....	54
Figure 25 - Spatial localization of Rec8 in oocytes arrested at MII. ....	56
Figure 26 - Spatial localization of Rec8 in oocytes fixed at AII. ....	57
Figure 27 - Spatial localization of Rec8 in oocytes fixed at TII. ....	58
Figure 28 - Spatial localization of Rec8 in oocytes fixed at Interphase. ....	58
Figure 29 - The effect of Demecolcine on Rec8 localization in oocytes fixed at AII. ....	59
Figure 30 - The effect of Demecolcine on Rec8 localization in TII eggs.....	60
Figure 31 - The effect of Demecolcine on Rec8 localization in oocytes fixed in Interphase.....	60

## Introduction

The efficiency of Somatic Cell Nuclear Transfer (SCNT) or animal cloning is extremely low. Typically, healthy progeny are produced from only 1-2% of reconstructed embryos (Kato *et al.*, 1998). This low efficiency may be due in part to the enucleation methods used in the cloning procedure. In traditional SCNT, oocytes arrested at metaphase of meiosis II (MII) are stained with Hoechst 33342 and exposed to UV irradiation to cause the fluorescence of the chromatin. Under constant UV exposure, the oocyte is punctured and its chromosomes are manually removed with a fine bore glass pipet creating an enucleated egg or cytoplasm. The cytoplasm is then injected with DNA or fused to a somatic cell. The reconstructed embryo is then stimulated to continue development into an embryo and beyond. This process is technically difficult, requiring expensive equipment and significant micromanipulation training. Additionally, not only is this a very labor intensive process, it is widely believed that, due to the invasiveness of this method, the egg may be irreversibly damaged beyond the point where healthy development can be sustained.

There are two main observations in support of this notion. Firstly, exposure to UV light has been shown to negatively affect oocyte competence in several species (Smith, 1993; Velilla *et al.*, 2002) by disturbing membrane processes, intracellular elements, and mitochondrial chromatin. Secondly, the manual removal of the MII chromosomes is imprecise. During this process, the meiotic spindle, the surrounding cytoplasm, and any other cellular components associated with the meiotic spindle like the anaphase-promoting complex (APC) are also removed from the egg. Unfortunately, many of these cytoplasmic components are crucial to the developmental competence of the enucleated oocyte and their removal has been demonstrated to reduce the cytoplasm's ability to support later development.

In order to increase the efficiency of SCNT, Baguisi and Overstrom (2000) reported the use of Demecolcine, a derivative of colchicine, to aid in the enucleation procedure. The MII oocytes were incubated in Demecolcine to depolymerize the meiotic spindle and the oocytes subsequently activated. It was observed that oocytes extruded the

chromatin in the second polar body with a high efficiency. Using this method, it was suggested that the karyoplast could then be removed more easily. Demecolcine-assisted enucleation has since been effective in several species including mice (Baguisi & Overstrom, 2000), sheep (Hou *et al.*, 2006), and cows (Russel *et al.*, 2005).

The APC is a multimeric protein complex that ligates ubiquitin chains to several protein substrates; thereby marking them for destruction by the 26S proteasome (reviewed by Castro *et al.*, 2005) and driving both the mitotic and meiotic cell through the cell cycle (reviewed by Zachariae & Nasmyth, 1999 and many others). *S. cerevisiae* mutants lacking various subunits of the APC have been shown to arrest in metaphase (Hartwell *et al.*, 1970). Additionally, the APC was required for the initiation of anaphase in *C. elegans* (Furuta *et al.*, 2000), yeast (Salah & Nasmyth, 2000), and mouse (Terret *et al.*, 2003). Since unsuccessful cloning attempts often fail to initiate anaphase (Overstrom Laboratory unpublished results), it is believable that the APC is somehow affected by the enucleation procedure. Therefore, the purpose of this project was to determine the effects of Demecolcine-induced microtubule depolymerization on the spatial localization of the anaphase-promoting complex (APC) and other markers of APC activity.

## Literature Review

### ***Animal Cloning Techniques***

Animal cloning or somatic cell nuclear transfer (SCNT) is the process by which an oocyte is enucleated, reconstructed with the DNA of another donor cell, and then stimulated to develop into a live organism. The overall goal of this process is to produce offspring with specific genotypic qualities identical to that of donor cells from a founder animal. SCNT has been successfully employed to produce a variety of organisms including sheep (Wilmot *et al.*, 1997), cows (Kato *et al.*, 1998), goats (Baguisi *et al.*, 1999; Lan *et al.*, 2006) and several others. However, nearly a decade after Wilmot *et al.* (1997) reported the birth of Dolly the sheep, the first live mammal cloned from an adult cell, the efficiency of this technique remains exceedingly low (2-5%) despite the variety of cloning methods employed (reviewed by Kato *et al.*, 1999; Campbell *et al.*, 2005).

### **Creation of a Cytoplasm**

There are three major steps in the production of a live mammalian clone: the generation of a cytoplasm, the reconstruction of an embryo, and activation/ subsequent development of the clone. The first step is the generation of a cytoplasm capable of epigenetically reprogramming a somatic cell genome to support the full development of a cloned offspring. To create a cytoplasm, the nucleus of an oocyte is removed. While oocytes can be gathered from slaughterhouses and matured in vitro (reviewed by Campbell *et al.*, 2005), such a procedure often leads to cytoplasm of reduced developmental competence (Wells *et al.*, 1997). Therefore, mature oocytes are most often harvested from hormonally primed individuals at the stage where the cell is naturally arrested at metaphase of the second meiotic division (MII). At MII, the DNA is tightly compacted along the metaphase plate at the center of the meiotic spindle, a microtubule complex that assists in the proper alignment and segregation of sister chromatids. To remove the DNA from the cell, the egg is punctured with a finely pulled needle and the entire meiotic spindle is aspirated along with variable amounts of the surrounding cytoplasm. Because the spindle complex is difficult to visualize under

standard bright field conditions, the DNA is typically localized by staining with a Hoechst dye and visualized by fluorescence microscopy. Unfortunately, UV exposure can damage mitochondria and several other membrane processes (Smith, 1993; Velilla *et al.*, 2002). Additional complexities of this technique include the requirement of specialized technical training on relatively expensive equipment (i.e. micromanipulator, inverted fluorescence microscope).

One alternative to the micromanipulation procedure is a technique developed by Vajita *et al.* (2001) called “handmade” cloning. In this system, the need for micromanipulators has been circumvented by the preparation and fusing of two half cytoplasts. Two oocytes were bisected and the portions with the nuclei were discarded. The remaining two halves were then fused with nuclei from a donor cell, creating a fully reconstructed embryo. While this is a simple alternative to conventional cloning, the low success rates still prevent this method from becoming economically viable.

Alternatively, Baguisi and Overstrom (2000) reported a method by which Demecolcine, a microtubule destabilizing agent, can aid in the enucleation process. MII stage eggs were activated and subsequently incubated in various agents affecting microtubule confirmation. 54% of eggs incubated in Demecolcine demonstrated induced enucleation, whereby the nuclear chromatin was extruded in the second meiotic polar body. Baguisi and Overstrom (2000) were then able to produce live healthy offspring from the generated cytoplasts, demonstrating the potential effectiveness of the chemically assisted enucleation approach.

## **Embryo Reconstruction**

The second step in the creation of an animal clone is the reconstruction of an embryo. To reconstruct an embryo, the DNA from the nucleus of a donor cell (karyoplast) must be stably incorporated within the new generated cytoplast. This is accomplished in one of several ways. The most common method is by electrofusion (reviewed by Ramos & Teissie, 2000). In this process, an electric field is applied to both the cytoplast and donor cell. Under specific electric conditions, the cell membrane of both “cells” will destabilize and, when brought into close contact with one another, the two membranes will merge. Thus, a newly reconstructed embryo is created with the

genetic material of the donor cell and the cytoplasm of an enucleated oocyte capable of epigenetic reprogramming.

In some species (like mice) where electrofusion is less effective, embryo reconstruction is accomplished by piezo injection (Chen *et al.*, 2004). According to EXFO, the maker of the PiezoDrill, high-frequency impulses are produced by a motor within the drill that travel longitudinally along an injection pipet. These impulses allow a glass pipet to pass through the zona pellucida and into the cytoplasm of the oocyte without destroying the cell membrane. The donor cell nucleus can then be injected directly into the cytoplasm creating a reconstructed embryo.

Another alternative to electrofusion is to use a non-touch laser to open a hole in the zona. The laser softens the membrane of the cell allowing for a blunt pipet (instead of a sharpened pipet) to be used for removal/ injection of chromatin. While no live offspring have yet been reported using this technology, advantages (as reported by Hamilton Thorne Biosciences- the maker of the XYClone Laser) include an increased speed and efficiency over traditional microinjectors and a resultant reduction in the trauma of the oocytes (Chen *et al.*, 2004; reviewed by Campbell *et al.*, 2005).

## **Activation and Development**

Following the reconstruction of the embryo, it is necessary to stimulate the egg to continue to grow and divide. Naturally, developing oocytes arrest at MII where they await an oscillating calcium signal caused by an invading sperm (reviewed by Jones, 2005). The calcium signal activates calmodulin-dependent protein kinase II which then activates the anaphase promoting complex to initiate the destruction of cyclin B, the regulatory element of Maturation Promoting Factor (MPF), and securin, an enzyme that prevents the premature cleavage of cohesion complexes, thus, allowing the cell to progress from meiosis into mitosis (Jones, 2005). This calcium signal can be mimicked artificially in many ways both chemically and electrically. In mice, the standard parthenogenetic activation stimulus is SrCl<sub>2</sub>. The strontium causes repetitive calcium transients to occur as organelle stores are released into the cytoplasm (Ibanez *et al.*, 2005). Ethanol has also been shown to activate mouse oocytes by causing the formation of inositol 1,4,5-triphosphate at the membrane and a concomitant influx of extra-cellular

calcium (Ibanez *et al.*, 2005). Ionomycin, a calcium ionophore, has also often been used in mice, sheep, and cows. Other reported parthenogenetic activation protocols include electroporation in media containing CaCl<sub>2</sub> or a microinjection of CaCl<sub>2</sub> into the cytoplasm (Machaty *et al.*, 1996).

Following activation and cleavage, embryos are transferred into surrogate mothers for development to term. While in some species, embryos can be immediately transferred into the host carrier, in most cases the embryos are developed in vitro to blastocyst stage prior to transfer. This allows for the morphologic selection of embryos before transplantation (Campbell *et al.*, 2005).

## ***Anaphase Promoting Complex Background***

### **APC in somatic cells**

The Anaphase Promoting Complex (APC) is a multi-subunit protein that is crucial in the regulation of the cell cycle (Peters, 2002) with subunit APC11 serving as the catalytic core (reviewed by Castro *et al.*, 2005). In somatic cells, the main function of the APC is the ubiquitination of cyclins (specifically cyclin B) and securin. Ubiquitin is a 76aa molecule that acts as a signal that causes the target protein to be transported to a proteasome for degradation (Chau *et al.*, 1989). The destruction of cyclin B leads to the inactivation of Cdk1, a cyclin-dependent kinase that initiates M phase in eukaryotic cells (Zachariae & Nasmyth, 1999). The inactivation of Cdk1 during anaphase and telophase is necessary for both the formation of prereplicative complexes and chromosome decondensation (Peters, 2002). Hence, the APC indirectly leads to the inactivation of Cdk1 by marking cyclin B for destruction.

The other main function of the APC in somatic cells is to label and destroy securin. Since securin binds and inhibits separase, its destruction indirectly activates the protease. Separase works to cleave SCC1 (Rec8 in meiotic cells), a subunit of the cohesion processes that hold sister chromatids together from metaphase until anaphase (Peters, 2002). Additionally, since Cdk1 initiatorily phosphorylates separase, the APC affects separase activity in two ways; by the reduction of cyclin B concentrations and the destruction of securin. (See Figure 1).

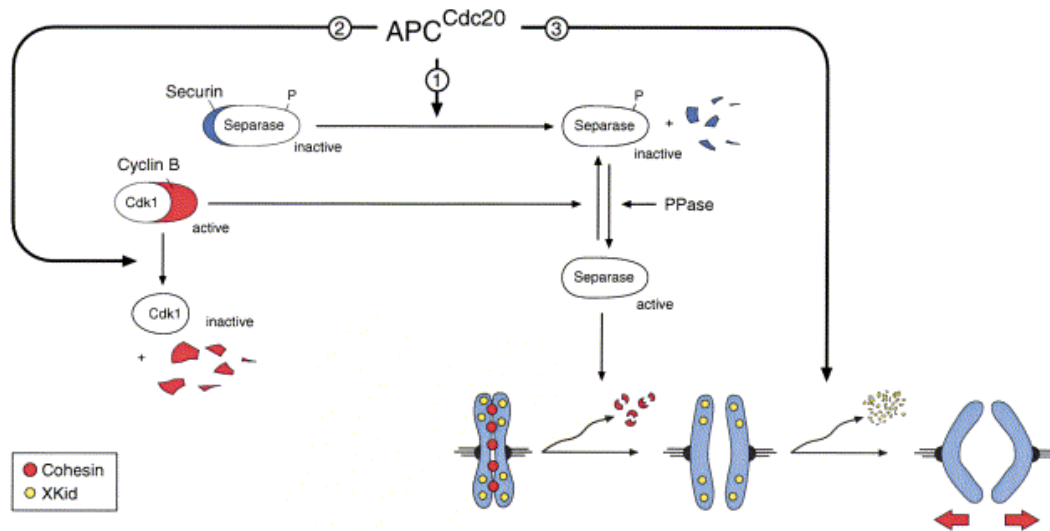


**Figure 1 - Initiation of Anaphase by the APC (Peters, 2002)**

The APC is activated at different parts of the cell cycle by the binding of Cdc20 and Cdh1. Early in mitosis when cdk activity is high, the APC binds Cdc20 and actively binds proteins with a destruction box (D-box), the aa sequence R-x-x-L-x-x-x-N/D/E common to all the substrates of APC<sup>cdc20</sup> (Harper *et al.*, 2002). APC<sup>cdc20</sup> degrades A-type cyclins during prometaphase and B type cyclins and securins during the beginning of metaphase (Peters, 2002). Alternatively, since Cdh1 is inhibited by cdk activity, the APC binds Cdh1 during G1, where cdk activity is low (see Figure 2). Similar to APC<sup>cdc20</sup>, APC<sup>cdh1</sup> also binds proteins with a specific sequence. That sequence, known as a KEN box (K-E-N-x-x-x-D/N) is common to all substrates of APC<sup>cdh1</sup> including Cdc20 (Peters, 2002). Accordingly, since APC<sup>cdh1</sup> is responsible for the destruction of Cdc20, it helps regulate the activity timing of APC<sup>cdc20</sup> (Harper *et al.*, 2002). Since APC<sup>cdc20</sup> and APC<sup>cdh1</sup> have different substrates, the APC has the ability to remain active throughout the changing conditions of the cell cycle.

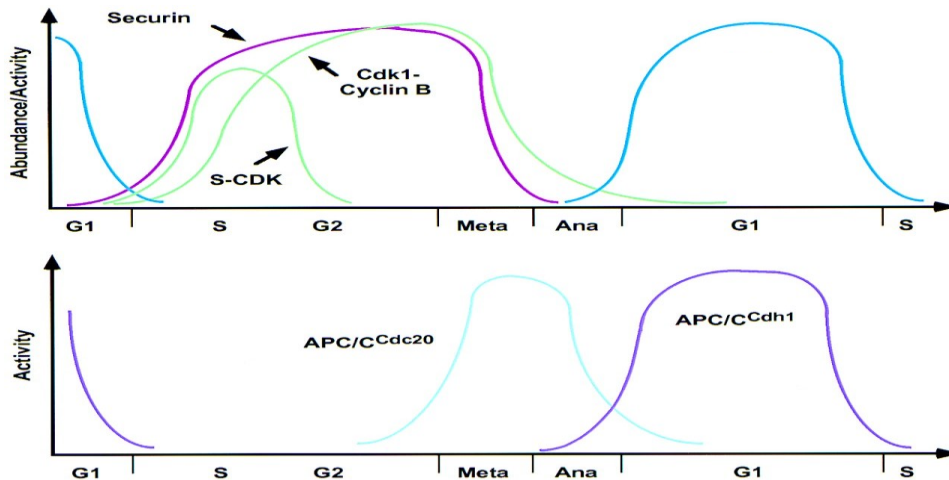


Figure 2 - APC activity (Zacharaie *et al.*, 1999)

## APC in M2 eggs

In normal vertebrate egg development, an egg will proceed through all of the steps of meiosis until it reaches a final step in which the cell can no longer advance without an external stimulus. This pause in development is known as the metaphase II (M2) arrest. This arrest is partially caused by cytotstatic factor (CSF) which inhibits the APC from degrading cyclin B. By maintaining high cyclin B-Cdc2 levels, the cells will remain at this arrest until fertilization. Upon fertilization, a series of  $Ca^{2+}$  signals initiate a cascade that ends in the destruction of cyclin B and the next cellular division (Nixon *et al.*, 2002). Experiments with cyclin B mutants without the D-box domain have shown that, if cyclin B is not degraded, no pronuclei will form and the cell will not exit meiosis after fertilization (Magdwick *et al.*, 2004).

Hysop *et al.* (2004) propose a model for mammalian eggs in which the  $Ca^{2+}$  signal affects the activity of the APC during a metaphase arrest and not the 26S proteasome as earlier characterized in lower organisms (Chiba *et al.*, 1999). Hysop *et al.* propose that the  $Ca^{2+}$  signal stimulates the loss of an APC inhibitor. One potential inhibitor Hysop *et al.* mentioned was Emi1 because of a potential phosphorylation site by CaMKII, the known  $Ca^{2+}$  transducer at fertilization (Markoulaki, 2003). However, Ohsumi *et al.* (2004) has reported that the M-phase arrest stimulated by Emi1 is separate from a CSF arrest in frogs (*Xenopus*). If Emi1 is not the APC inhibitor, it is also possible that CSF may be a novel  $Ca^{2+}$ -dependent inhibitor of the APC (Hysop *et al.*, 2004).

During metaphase, securin maintains the inactivity of separase, an anaphase specific protease, until all the chromosomes are properly aligned or the initiation of anaphase (Wirth *et al.*, 2006). At the onset of anaphase, the destruction of securin (regulated by APC ubiquitination) allows separase to cleave the SCC1 subunit (Rec8 in meiotic cells) of cohesion, thus allowing sister chromatids to separate.

## **APC Subunits**

### **Apc11/Apc2 as the catalytic core**

The cullin-RING subunits Apc2 and Apc11 of the APC are believed to be the catalytic core of the complex (Gmachl *et al.*, 2000; Levenson *et al.*, 2000; Tang *et al.*, 2001). Although Apc11 is among the smallest of the APC subunits discovered (Passmore *et al.*, 2005) Gmachl *et al.*, (2000) have shown that recombinant human Apc11 and only Apc11 (not any of the other known subunits of the APC) is sufficient for the synthesis of multiubiquitin chains *in vitro* in the presence of an E1 enzyme, Ubc4 and an ATP regenerating system. This synthesis occurred in both the presence and absence of substrates. However, these chains were non-specific as a D-box mutant of securin was ubiquitinated as well as the wild type securin. Additionally, Tang *et al.* (2001) coinfecting Hi5 insect cells with viruses containing 10 APC subunits. Combined, the multiple baculoviruses conveyed ubiquitin ligase activity. This activity was lost if only Apc2 or Apc11 were removed. Furthermore, Tang *et al.* (2001) showed that the Apc2/11 complex is sufficient for the ubiquitination of securin with UbH10 as the E2 enzyme. Tang *et al.* (2001) then showed that while Ubc4 can interact directly with the RING of Apc11, UbH10 binds Apc2 strongly and Apc11 weakly.

### **Structure of Apc11 RING finger**

The E3 ubiquitin ligase activity of the APC is conveyed by two Zn<sup>2+</sup> ions binding within the RING domain of Apc11 and perhaps partially a third Zn<sup>2+</sup> outside of the RING motif (Tang *et al.*, 2001). When coordinating with these Zn<sup>2+</sup> ions, a stable tertiary RING structure is formed. This RING structure is necessary for the ubiquitination of APC substrates as mutants with disrupted ring structures show significantly reduced to no ubiquitin ligase capability (reviewed by Peters, 2002). Although Tang *et al.*, (2001) demonstrated that high levels of Zn<sup>2+</sup> alone can catalyze minimal levels of a ubiquitination reaction in the presence of an E2, it is not yet known whether the RING

structure of the APC directly catalyzes the ligase reaction through the Zn ions or whether it allows for a stable proximity reaction to occur (Passmore & Barford, 2004).

## **Structure of Apc2**

As the second largest protein of the APC (Jorgensen *et al.*, 2001), Apc2 is a protein with a cullin C-terminal homology region that binds strongly to Apc11 (Tang *et al.*, 2001). All cullin proteins form a rigid scaffolding-like structure by binding the RING with their C-terminal domain while the N-terminal region is thought to actively recruit the E2 enzymes (reviewed by Petroski & Deshaies, 2005). The structure of Apc2 has been inferred from its homology to Cull1, another cullin protein in the SCF E3 ligase (Zheng *et al.*, 2002). This inference is further supported by the fact that, while the sequence homology of the two proteins is mainly restricted to the C-terminal cullin domain (Passmore, 2004), a crystal structure of the C-terminal 78 aa (well outside of the cullin region) forms a hinged-helix that can be superimposed over the same Cull1 region (Zheng *et al.*, 2002). Along the C-terminus, Cull1 forms a V-shaped groove that binds Rbx1, a RING finger protein comparable to Apc11 (Zheng *et al.*, 2002). Along its N-terminus, Cull1 contains several helical repeats that are arranged to allow for the binding of Skp1, a linker protein that binds substrates of the SCF containing an F-box.

## **Apc10 (Doc1)**

Apc10 is required for E3 ligase activity on certain substrates and plays a specific role in substrate recognition (Passmore *et al.*, 2003). Apc10 interacts directly with Apc11, the catalytic core of the APC (Tang *et al.*, 2001). Mutants of both fission and budding yeast lacking Apc10 show an arrest at metaphase and the accumulation of mitotic cyclins (Kominami *et al.*, 1998). Apc10 is the first member described in the Doc homology family, a group of proteins that have been detected in other E3 ligases unrelated to the APC (reviewed by Passmore, 2004). Although its specific role is still undefined, Passmore *et al.* (2003) proposed that, since Apc10 mutants have a diminished ability to bind substrates, it functions as a regulator of substrate recognition. An

additional report by Carroll & Morgon (2002) shows that Apc10 increases processivity, the addition of multiple ubiquitin molecules in a single binding event, by reducing substrate disassociation.

### **Apc1 (Tsg24)**

Apc1 is the largest subunit of the APC (reviewed by Castro *et al.*, 2005) and transiently localizes to the centromeres of mammalian chromosomes (Jorgenson *et al.*, 1998) during mitosis in CHO cells and throughout the cell cycle in murine cells. Its homologues include BimE from *Aspergillus nidulans* and Cut4 from *Schizosaccharomyces pombe* (reviewed by Castro *et al.*, 2005). The predicted 3D structure contains Rpn1 and Rpn2, repetitive motifs that form a horseshoe-like structure (Jorgensen *et al.*, 2001). While the exact function of this repetitive sequence is unknown, it has been predicted that this horseshoe might play a role in binding unfolded proteins or as a scaffold for the rest of the APC (Lupas *et al.*, 1997).

### **Tetratricopeptide TPR repeats (Apc3, Apc6, Apc7, Apc8)**

The TPR sequence motif is found in proteins with various biochemical activities and is thought to mediate protein-protein interactions (Castro *et al.*, 2005). TPR sequences arrange themselves into anti-parallel  $\alpha$ -helices that combine to form a right handed super helix (Das *et al.*, 1988). With specific aa residues on the outside and an extended groove inside the superhelix, the structure of multiple TPR sequences allows for the assembly of multi-protein complexes and the binding of an  $\alpha$ -helix in the center. Specifically, Vodermaier *et al.* (2003) showed that Apc3 and Apc7 bind to the c-terminal isoleucine-arginine (IR) region of both Cdc20 and Cdh1, key activators of the APC. Since all these TPR subunits are phosphorylated during mitosis and that phosphorylation is necessary for the activation of the APC, it is presumed that this phosphorylation event increases the binding ability of the APC to Cdc20 (Kraft *et al.*, 2003; reviewed by Castro *et al.*, 2005). Interestingly, Apc10 also contains an IR tail signifying that Apc10

association is also mediated by the TPR subunits. Apc7 has only been described in vertebrates.

### **Apc4, Apc5**

Less is known about these subunits. It is hypothesized that these subunits along with Apc1 connect Apc2 and Apc11 to the TPR subunits (Vodermaier *et al.*, 2003).

### **Apc9, Cdc26**

Little is known about these two subunits other than the fact that they are required for overall structure of the APC. Apc3 concentration is reduced in Apc9 and Cdc26 mutants while Apc6 and Apc9 are reduced in Cdc26 mutants. So far, Apc9 has only been described in yeast.

### **Apc13(Swm1), Apc14, Apc14(Mnd2)**

Apc13, Apc14, and Apc15 are subunits that have only been described in yeast. While the biochemical function of these subunits is still unclear, it is hypothesized that they help maintain the structure of the APC. Because the gene for Apc13 and Apc15 were originally identified in meiotic screens (Ufano *et al.*, 1999; Rabitsch *et al.*, 2001), a role for Apc13 and Apc15 in meiosis has been predicted.

### **Cdc20 (Fizzy)**

Cdc20 binds to the APC during mitosis. Once bound, the APC becomes activated to ubiquitinate substrates containing a D-box, a short aa sequence that promotes APC recognition. The degradation of these substrates including securin, Xkid, and several cyclins drives the cell through the mitotic cycle.

## ***APC localization and activity***

Previously, mitotic APC localization has been observed in vitro (Tugendreich *et al.*, 1995; Kraft *et al.*, 2003; Acquiviva *et al.*, 2004). The staining of *apc6* and *apc3* appears primarily on the centrosome at all cell cycle stages and coupled with the spindle following nuclear envelope breakdown (Tugendreich *et al.*, 1995). During interphase, *Apc3* staining localized mainly to the nucleus and bound to the kinetochores in prophase. At pro-metaphase, the staining appeared on the spindle (poles and fibers) and on the centromeres of chromatids that had not yet aligned on the metaphase plate (Acquiviva *et al.*, 2004). Acquiviva *et al.* (2004) went on to show that *Apc3* localization could be eliminated in mutant cells without an active spindle checkpoint.

It is widely believed that *Apc3* localization is necessary for the function of the APC (reviewed by Pines & Lindon, 2005). One proposed mechanism of the RING E3 ubiquitin ligases (including the APC) is that of a molecular scaffold. As the E3 binds both the E2 enzyme (ubiquitin conjugating enzyme) and the substrate, it brings specific lysine residues on the substrate into close proximity with an activated ubiquitin molecule (reviewed by Passmore & Barford, 2004). Additionally, Clute & Pines (1999) demonstrated that cyclin-B1 degradation occurs at the same location as APC localization in HeLa cells.

## ***Cytoskeleton Affecters***

The cytoskeleton is composed of three types of protein filaments: actin filaments, microtubules, and intermediate filaments (IFs).

### **Intermediate Filaments**

Intermediate Filaments (IFs) have a diameter of ~10nm with an amino-terminal head, a central rod domain, and a carboxy-terminal tail. These non-polarized filaments typically play structural or tension bearing roles in the cell. The 4 types of IFs are keratin filaments (acidic and basic), vimentin-related filaments, and neurofilaments. While most IFs form apolar tetramers of anti-parallel dimers, lamins combine to form the 2D lattice of the nuclear lamina. These lamins are broken down by cell cycle kinases upon entry into M-phase (Lodish *et al.*, 1999).

### **Microfilaments**

Microfilaments (actin filaments) are composed of actin monomers (G-actin) that bind ATP and link together in a head-to-tail manner to form long polarized filaments with a diameter typically between 5 and 9 nm (Lodish *et al.*, 1999). These long filaments (F-actin) have a negative and a positive end. At the positive end, monomer addition occurs quickly while very little polymerization occurs at the negative end. Once the filament reaches a steady-state length, ADP-bound monomers will separate from the minus end at the same rate as ATP bound monomers are added to the positive end. This process is called treadmilling.

There are several drugs and proteins that affect microfilament characteristics. The Cytochalasins are a group of fungal molecules that bind to the positive end of F-actin and prevent further addition of G-actin. However, depolymerization at the minus end can still occur, thus leading to the overall depolymerization of the filament (Fementek fact sheet

on Cytochalasin [<http://cytochalasin.4mg.com/>]). Since Cytochalasin D, produced by *Zygosporium mansonii*, has been known to affect only the microfilament system and not the glucose transport system, it has become widely used in cellular manipulation techniques. The concentration required for half-maximal inhibition with Cytochalasin D is  $20^{-8}$  M (Brown & Spudich, 1979). Cytochalasin D is soluble in methanol, ethanol, and DMSO and requires  $-20^{\circ}\text{C}$  for long-term storage. While both Cytochalasin D and Cytochalasin B inhibit actin function, Cytochalasin D is about 10-fold more potent than Cytochalasin B (Brown and Spudich, Figures 1&2, 1979). Other Cytochalasins include Cytochalasin A,B,C, and E. Cytochalasin A, isolated from *Drechslera dematoidea*, acts as an inhibitor of glucose transport, actin polymerization, and microtubule formation. Cytochalasin B, also isolated from *Drechslera dematoidea* inhibits microfilament formation at 1 microgram/ml but at higher concentrations (about 5 g/ml) it begins to inhibit glucose transport (Fementek fact sheet on Cytochalasin [<http://cytochalasin.4mg.com/>])). Cytochalasin C, isolated from *Meterrhizium anisopliae*, acts as a potent inhibitor of actin filament and contractile microfilaments. Cytochalasin E, isolated from *Aspergillus clavatus* inhibits angiogenesis and tumor growth by inhibiting F-actin formation in blood platelets.

Phallotoxins are members of group of bicyclic heptapeptides isolated from the mushroom *Amanita phalloides* (Cooper, 1987). In particular, Phalloidin binds along the sides of the microfilaments and prevents actin filaments from depolymerizing, thereby lowering the G-actin concentration needed for F-actin to form (Cooper, 1987). Phalloidin, supplied as a dried residue, is best dissolved to a concentration of 0.1 mg/ml in methanol (Small *et al.*, 1999). Depending on its conjugation, it can be stored at  $-20^{\circ}\text{C}$  for several months. A ratio of one Phalloidin molecule to every 1.7 actin promoters has been shown to be adequate for maximal depolymerization protection, with a disassociation constant of 85nM (reviewed by Cooper, 1987). Fluorescently tagged Phalloidin (AlexaFluor 488 Conjugate available online [<http://www.cambrex.com/>]) has also been used to label F-actin. Using tagged Phalloidin in excess to the binding sites allows for a quantitative measurement of the total amount of F-actin in a cell (Cooper, 1987).

Jasplakinolide (<http://www.emdbiosciences.com/>) isolated from the sea sponge *Japis johstoni*, induces actin polymerization in vitro and competitively inhibits Phalloidin binding (Bubb *et al.*, 1994) with a disassociation constant of 15nM. This drug can be purchased as a powder or in a 1mM solution of DMSO from EMD or Molecular Probes (Eugene,OR) and must be stored at -20°C to be stable for 3-4 months. In their actin-binding studies, Bubb *et al.* (2000) determined that Jasplakinolide not only has the ability to bind F-actin faster than they were able to mix their samples, but also reduce the critical concentration of actin in a dose response manner (6-fold decrease at 0.15uM Jasplakinolide and 20-fold decrease at 0.3uM Jasplakinolide).

Dolastatin 11, isolated from the mollusk *Dolabella auricularia*, also helps to stabilize F-actin in vitro (Oda *et al.*, 2003). For research use, this protein must be isolated or synthesized in house (Bai *et al.*, 2001). This protein binds actin at a different site than Phalloidin and Jasplakinolide. When comparing the effects of Dolastatin 11 with those of Jasplakinolide, minor microfilament destabilization occurred with both drugs at 30 min, and extensive destabilization occurred by 60 min (Bai *et al.*, 2001). In a study comparing the effects of several drugs on f-actin in vitro, Bai *et al.* (2001) observed clear stimulatory effects at 10uM with Dolastatin 11 and Jasplakinolide, and modest stimulation with Phalloidin.

Gelsolin is a protein found in many eukaryotic organisms including plants, lower eukaryotes, and vertebrates (for review see McGough *et al.*, 2003). In the presence of calcium, Gelsolin can cut an actin filament and cap it on the plus (barbed) end, preventing the addition of G-actin. This severing effect is inhibited by Phalloidin (Way *et al.*, 1992). Without the addition of G-actin to the plus end the minus end of the microfilament can slowly depolymerize. Additionally, Gelsolin has the ability to nucleate G-actin and begin the process of polymerization into F-actin if the concentration of G-actin is above a critical concentration. Either human or bovine lyophilized gelsolin (<http://www.sigmaaldrich.com/>) should be stored at -20°C. Once dissolved in water, the solution is stable at 4°C for 1 week.

By binding to the sides of F-actin, Cofilin family members, including actin depolymerization factor (ADF), can cause the actin filament to twist improperly, disrupting the Phalloidin binding site. Often this twisting breaks the filament and prevents further lengthening (for review see Bamburg, 1999). Below pH 7, Cofilin increased the unassembled actin pool while co-sedimenting with F-actin. Depending on the pH, Cofilin can depolymerize filaments at different rates. Although Cofilin has been shown to increase the growth rate at the plus end, it increases the off rate at the minus end much more significantly (10 fold vs. 20-40 fold). The critical concentration of human Cofilin to increase the G-actin concentration has been shown to be <2uM (Hayden *et al.*, 1993). Recombinant chicken Cofilin (purchased from [<http://www.sigmaldrich.com/>]) can only be stored at 4°C for a few days but lyophilized Cofilin (before being dissolved in dH<sub>2</sub>O) can be stored at -20°C for 6 months.

## **Microtubules**

Microtubules are long tube-like structures made up of repeating heteromers of alpha and beta tubulin. The walls of these microtubules are ~5nm wide while the entire diameter of the structure is around 25nm wide (Lodish *et al.*, 1999). Like microfilaments, these structures are also polarized with a fast growing, positive end and a slower negative end. Often the minus end is anchored to the centrosome in animal cells. Microtubules comprise the mitotic spindle which is well known for its appearance and disappearance during the cell cycle. This polymerization/depolymerization cycle is closely related to beta tubulin's ability to bind and utilize GTP. As more GTP is converted to GDP, the bonds of polymerization grow weaker, so the microtubules either grow slowly at the positive end or quickly degrade (Johnson, 2003). Similar to microfilaments, microtubulins have also been known to undergo treadmilling (Wilson *et al.*, 1999). While modifications to microtubules like acetylation help stabilize the protein complex, the foremost regulators of microtubule stability are proteins called Microtubule-Associated Proteins (MAPs) including MAP-1, MAP-2 and tau, which can either promote the degradation of tubulin complexes or help to maintain the polymerized state.

Colchicine, Demecolcine (Colcemid<sup>TM</sup>), and Nocadazole all prevent microtubule polymerization by binding to tubulin at the plus end and not permitting further addition of protofilaments (Wilson *et al.*, 1999; [<http://cellbio.utmb.edu/>]).

Colchicine, isolated from the saffron plant, *Colchicum autumnale*, is an alkaloid that has the ability to stabilize the plus ends of microtubules greatly reducing the percentage of catastrophic collapse (Wilson *et al.*, 1999). The binding event of Colchicine to tubulin is a two-step process. First, a pre-equilibrium complex forms between the two proteins. This step represents a reversible, low-affinity binding event. After this pre-complex forms, the proteins undergo a slow period of distinct conformational changes until they form the final TC complex. In this form, the binding of Colchicine and tubulin is nearly irreversible. Once bound to the end of microtubules, the TC complex inhibits growth of that microtubule. This does not mean, however, that the microtubule ends are no longer competent to grow, as TC complexes can still attach to the plus ends of the microtubule (Wilson *et al.*, 1999). The effects of Colchicine can occur at low concentrations, with only 1-2 molecules of Colchicine per microtubule reducing the rate of tubulin addition by 50%. Additionally, at concentrations of 0.1-1 µg/ml, Colchicine can cause the mitotic arrest of dividing cells (Sigma product sheet available online [<http://www.sigma.com/>]). Colchicine is soluble in water, chloroform, benzene and can be autoclaved in solution for sterilization. It can be stored in the dark for up to 6 months.

Demecolcine (Colcemid<sup>TM</sup>) is the methylated derivative of Colchicine that has been shown to arrest cells in metaphase (Sigma product sheet available online [<http://www.sigma.com/>]). It produces this effect because it depolymerizes microtubules and inhibits microtubule formation, thus inactivating the spindle arresting chromosomes at the metaphase plate (Calibochem product sheet available online [<http://www.emdbiosciences.com/>]). Because the cell cycle will continue normally once Demecolcine is removed, Demecolcine is readily reversible. It is soluble in ethanol, chloroform, and DMSO to 10mg/ml. Demecolcine is stable as a powder at room

temperature for 3 years. When reconstituted, Demecolcine should be stored frozen at -20°C for 6 months.

Nocodazole arrests mitotic cells at the G<sub>2</sub>/M transition by depolymerizing microtubules in interphase and mitotic cells which arrests the cells. Although Nocodazole is a competitive inhibitor of the binding between Colchicine and tubulin (Jordon *et al.*, 1998), unlike Colchicine, the effects of Nocodazole are rapidly reversible (Vasquez *et al.*, 1997). Nocodazole increases the GTPase activity of tubulin by nearly five-fold. This heightened activity increases the concentration of tubulin dimers in solution and thereby increases the rate of addition of these tubulin dimers to the microtubule. The nature of the adjacent nucleotide bound at next to the tubulin dimer then determines whether the microtubule continues to grow (more slowly than before), pauses, or collapses (Vasquez *et al.*, 1997). The solubility of Nocodazole is 10mg/ml in DMSO (Sigma product information sheet). When stored at 2°C the powder is stable for two years. When reconstituted in media, Nocodazole is stable for 1 week. Also, Nocodazole has been demonstrated to act much faster than other microtubule depolymerizing agents like Demecolcine.

Isolated from the periwinkle plant *Catharanthus roseus*, Vinblastine is a vica-related drug that does not compete for the Colchicine site on tubulin (Jordon *et al.*, 1998). Despite this fact, Vinblastine, at low concentrations (<uM), affects microtubule dynamics in a manner similar to Cholchicine. At a concentration of only 1-2 Vinblastine molecules per microtubule, Vinblastine inhibits polymerization at the plus end by 50% (Wilson *et al.*, 1999) without significantly depolymerizing the microtubule. Additionally, by binding tubulin, Vinblastine changes the confirmation of the tubulin molecule. This conformational change causes an aggregation of tubulin that, like Colchicine, reduces the catastrophe frequency and increases the rescue frequency of the microtubule (Wilson *et al.* 1999). At a higher concentration (>5uM), Vinblastine will depolymerize the microtubules by removing tubulin monomers from both the plus and minus ends. At an even higher concentration (>100uM), paracrystalline arrays of bound drug and tubulin form both in vitro and in vivo. Vinblastine Sulfate salt (purchased form Sigma) is

soluble to 20mg/ml in methanol and will remain stable at room temperature for two years. Fluorescently tagged Vinblastine (Invitrogen) can be useful for labeling B-tubulin.

Paclitaxel (aka Taxol), isolated from the needles of *Taxus brevifolia*, stabilizes microtubules in vitro. In the presence of Paclitaxel, microtubules become resistant to the depolymerization effects of calcium, cold, dilution, and many destabilizing drugs (fact sheet available 5/15/05 [<http://probes.invitrogen.com/>]). By binding the inside of microtubules (via pores in the surface), Paclitaxel stimulates microtubule polymerization. Paclitaxel also has the ability to promote nucleation of microtubules and reduce the critical concentration of tubulin to nearly zero at equilibrium (Wilson *et al.*, 1999). Cells incubated with Paclitaxel are halted in the G2 or M phase of the cell cycle (fact sheet available 5/15/05 [<http://probes.invitrogen.com/>]). Unlike Demecolcine, the effects of the drug persist well after the removal of the agent from the system. Paclitaxel is soluble in DMSO, MeOH, and EtOH and should be stored at -20°C protected from light for no more than a month. Invitrogen offers several Paclitaxel conjugates that will fluoresce in either the green, red, or orange range. A typical working concentration of unlabeled Paclitaxel is 0.1uM and 1uM for labeled Paclitaxel.

## **Materials and Methods**

All animals were handled under the strict guidelines dictated by the Institutional Animal Care and Use Committee (IACUC) of Worcester Polytechnic Institute.

### ***Oocyte collection***

In order to induce superovulation in donor mice, female CF-1 mice (Charles River Laboratories) of breeding age were injected with Pregnant Mare Serum Gonadotropin (PMSG, Calbiochem) and Human Chorionic Gonadotropin (hCG, Calbiochem). For both hormones, 5IU was administered per mouse via intraperitoneal injection. PMSG was injected 64 hours before collection and hCG was given 48 hours later. Oviducts were dissected from mice euthanized by CO<sub>2</sub> asphyxiation and placed in FHM media (Chemicon, see APPENDIX for composition) at 37°C. Oocytes were separated from surrounding cumulus cells by a brief exposure to bovine hyaluronidase (HA, Sigma, 150units/ml, <10 minutes). Oocytes with poor morphology (lysed, fragmented, dark pigmentation) were discarded. Oocytes were washed three times in FHM media and randomly sorted into treatment groups. Some oocytes were immediately fixed (see below) at metaphase of meiosis II (MII).

### ***Oocyte activation***

Oocytes were activated with either a 5 minute incubation in 7% ethanol or a continuous exposure to 10mM strontium chloride (SrCl<sub>2</sub>, Sigma), and fixed at specific points in development.

For ethanol activation, all procedures were accomplished at 37°C. Denuded oocytes were washed 3 times in FHM and transferred to FHM containing 7% absolute ethanol. After 5 minutes, oocytes were washed 4 times with FHM, 3 times in KSOM (+aa, Chemicon, see APPENDIX for composition), and incubated in KSOM at 37°C in 5% CO<sub>2</sub>. After 10 minutes, some oocytes were transferred to FHM containing 0.4ug/ml Demecolcine (Sigma).

For SrCl<sub>2</sub> activation, the denuded oocytes were washed 3 times in FHM, 3 to 4 times in KSOM (without Ca<sup>+2</sup>, Chemicon, see APPENDIX for composition) equilibrated to 37°C in 5% CO<sub>2</sub>, and then incubated in KSOM containing 10mM strontium chloride at 37°C with 5% CO<sub>2</sub>. After 15 minutes, some oocytes, depending on experimental design, were transferred to KSOM containing both SrCl<sub>2</sub> (10mM) and Demecolcine (0.4ug/ml) and incubated at 37°C with 5% CO<sub>2</sub>.

### **Oocyte fixation**

Depending on experimental requirements, oocytes were either fixed at metaphase of meiosis II (MII) immediately following the FHM wash or activated and fixed at t=25 minutes, t=125 minutes, t=245 minutes for anaphase II, telophase II, and interphase respectively. The initial exposure to EtOH or SrCl<sub>2</sub> was considered T<sub>0</sub>. For comparison purposes, oocytes were fixed in either 2% paraformaldehyde (PFA) solution containing 0.1% Triton X-100 or Microtubule Stabilization Buffer- Extraction Fixative (MTSB-XF, see APPENDIX for composition; (Mattson *et al.*, 1990)). Oocytes remained in fix solution for a minimum of 30 minutes at 37°C and then transferred to Blocking Buffer (block, Allworth & Albertini, 1993; see APPENDIX for composition) for storage at 4°C.

### **Oocyte staining and imaging**

To localize Apc11, a polyclonal antibody raised in rabbits against N-terminal amino acids of human APC11 (Santa Cruz) was used as a primary antibody. Oocytes were then washed 3 times with Phosphate Buffered Saline containing 0.1% Polyvinylpyrrolidone (PBS/PVP, Sigma) at room temperature and blocked with Blocking Buffer (block) for at least 30 minutes at room temperature. Apc11 was then probed with a goat anti-rabbit IgG antibody labeled with Alexa fluor 488 (5ug/ml in Blocking Buffer, green, Molecular Probes) and extensively washed with PBS/PVP. Microtubules were localized using a 1:1 mixture of primary monoclonal antibodies raised against  $\alpha$ -tubulin and  $\beta$ -tubulin (Sigma, 1:1000 dilution in Blocking Buffer, see APPENDIX), washed 3 times with PBS/PVP, blocked for at least 30 minutes with Blocking Buffer, and visualized with a goat anti-mouse IgG<sub>1</sub> secondary antibody labeled with Alexa fluor 594

(5ug/ml in Blocking Buffer, red, Molecular Probes). Oocytes were subsequently washed with PBS/PVP and chromatin was visualized by exposure to Hoechst 22358 (10ug/ml in block, blue, Molecular Probes). Oocytes were mounted on glass slides in 25ul mounting solution (50% glycerol, 50% PBS, 25mg/ml sodium azide), covered with cover glass (22x22mm, #1, Fisher Scientific), and sealed with clear nail polish (New York Color Inc.). Imaging was accomplished on a Zeiss Axiovert 200M inverted fluorescence microscope coupled to a Roper CoolSnapFx camera through a 63x oil emersion objective and 10x eyepiece/camera lens. Metamorph and Axiovision image processing software was used to collect micrographs.

To visualize Cdc20, the protocol was similar to the visualization of Apc11 with different antibodies. The anti-cdc20 antibody (Santa Cruz) was raised in rabbits against amino acids mapping to the N-terminal of human p55 (CDC20). The secondary was a goat anti-rabbit IgG labeled with Alexa fluor 594 (5ug/ml in Blocking Buffer, red, Molecular Probes). Since a red Alexa 594 secondary was used to label cdc20, the tubulin secondary was switched to goat anti-mouse IgG<sub>1</sub> labeled with Alexa fluor 488 (5ug/ml in Blocking Buffer, green, Molecular Probes).

For Rec8 staining, a similar procedure was followed. The polyclonal anti-Rec8 was raised in goats against amino acids mapping to the N-terminus of human Rec8 (Santa Cruz Biotech., sc-15152). The secondary was a donkey anti-goat IgG labeled with Alexa 594 (5ug/ml, red, Molecular Probes). Tubulin visualization was accomplished using Alexa fluor 488 (5ug/ml, green, Molecular Probes) as a secondary. To reduce tubulin staining, the  $\alpha\beta$ -tubulin cocktail was used at a 1:2000 dilution throughout the Rec8 staining protocol. In order to avoid non-specific binding, the blocking solution used throughout Rec8 staining contained no goat serum (see APPENDIX for complete composition).

A minimum of 10 eggs were imaged for every treatment with each antibody. Unless otherwise stated, all images presented were representative of the group with little egg to egg variation.

## ***Antibody optimization***

Because the three primary antibodies have not been well characterized in mouse oocytes, it was first necessary to optimize the staining protocol. The same optimizing protocol was followed for each antibody.

## **Hela cell culture**

The first step in the optimization process was to determine the localization pattern in HeLa cells. The HeLa cell culture was grown according to ATCC biosafety level 2 regulations in Minimum Essential Media, Eagle Salts (EMEM) with 10% Fetal Bovine Serum and penicillin/streptomycin at 37°C under 5% CO<sub>2</sub>. When cells were at or above 85% confluence, cultures were split 1:8. Cells were seeded on glass slides at 25% confluence, synchronized with a Thymidine/ Hydroxyurea protocol according to Takita *et al.* (2003), and fixed in MTSB-XF for 1 hour at room temperature. Detailed split and synchronization protocols can be found in the APPENDIX. Fixed cells were stored in Blocking Buffer at 4°C.

Synchronized and unsynchronized cells were stained for the presence and localization of Apc11, Cdc20, or Rec8. Initially, cells were incubated in varying concentrations of each primary antibody (1:1000, 1:500, 1:200) for 1 hour at room temperature. The cells were washed 2 times with PBS/PVP and incubated in the corresponding secondary antibody tagged with Alexa fluor 594 (5ug/ml in Blocking Buffer) for 1 hour at room temperature. The cells were then washed again and subjected to a brief (~15 minutes) incubation in Hoechst 22358 (1µg/ml) to stain DNA. As negative controls, some cells were incubated in PBS in lieu of either primary or secondary antibody.

## **Concentration study**

Once an ideal concentration was determined in HeLa cells, this information was used to optimize the staining protocol for mouse oocytes. All optimization studies were conducted with oocytes arrested at MII and randomly assorted into treatment groups.

The same optimization procedure was followed for Apc11, Cdc20, and Rec8. Oocytes were incubated in one of several concentrations of primary antibody (1:100, 1:200, 1:500, 1:1000, 1:2000, 1:4000 in Blocking Buffer) before being imaged. Additionally, the incubation time and temperature was varied (1 hour at room temperature, 1 hour at 37°C, overnight at 4°C). As negative controls, Blocking Buffer was substituted for either primary or secondary antibody for some oocytes. Following the incubations, the oocytes were imaged and the optimal protocol was determined (listed previously in Materials and Methods).

Following the concentration study, it was determined that an incubation in a 1:2000 dilution of anti-Apc11 overnight at 4°C was optimal for Apc11 localization. For Cdc20, a 1 hour incubation at room temperature in 1:250 was ideal. For Rec8, a 1:100 dilution of primary antibody in Blocking Buffer was used.

## Results

### ***Part I: Antibody validation***

Since the localization of the Anaphase Promoting Complex, specifically subunits Apc11 and Cdc20, has not been well studied in mouse oocytes, it was first necessary to validate the antibodies in a well characterized system like HeLa cells. Cells fixed in MTSB-XF were stained for either Apc11 or Cdc20 (*red*) and counterstained with Hoechst 22358. As a negative control, some cells underwent an identical staining procedure substituting blocking solution for the secondary antibody (Figure 3A-C) or primary antibody (Figure 3D). Cells in negative control experiments appeared as dull, non-distinct red hazes (Figure 3).

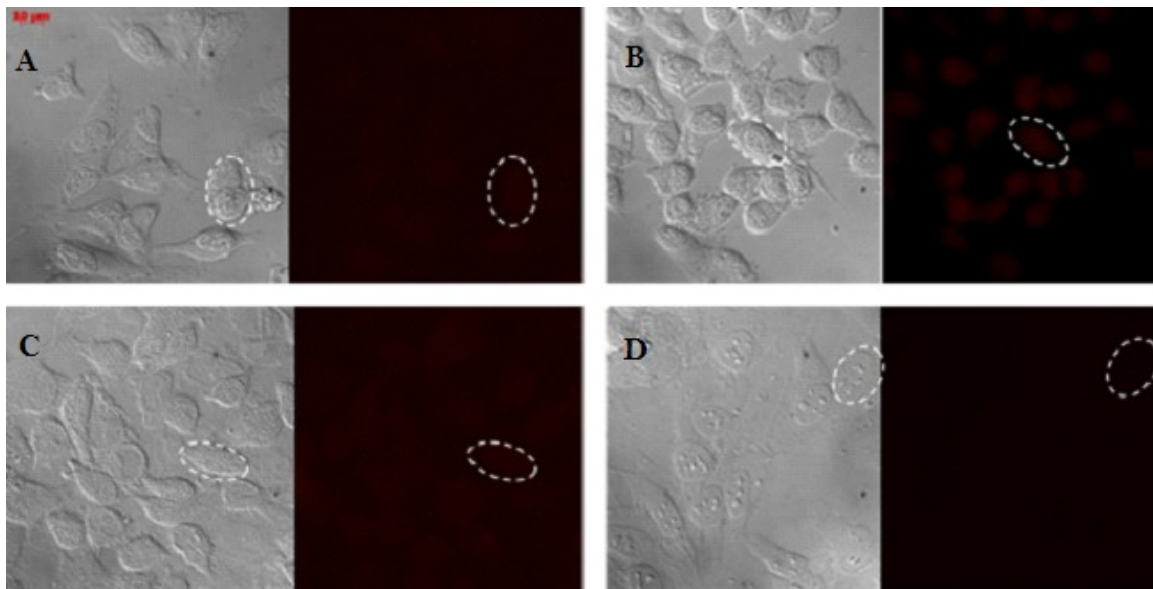


**Figure 3 - Negative control images of HeLa cells**

Unsynchronized HeLa cells were imaged without secondary or primary antibodies in the staining protocol: Apc11 alone (A), Cdc20 alone (B), Rec8 alone (C), or Alexa594 Goat anti-Rabbit IgG alone (D). DIC images (left) are shown with 5ms exposure; Red fluorescence images (right) are shown with a 100 ms exposure. Single cells are circled with a white dash. The background has been set to black.

In non-dividing ( $G_2$ ) cells, Apc11 appeared both cytoplasmically and in the nucleus (Figure 4A). However, the staining pattern was quite different in dividing cells. Apc11 colocalized with the kinetochores during prophase (*orange arrows*) and the

mitotic spindle during metaphase (*yellow arrow*). This result is consistent with the report of Acquaviva *et al.* (2004), who demonstrated a similar localization for Apc3 (Figure 5).

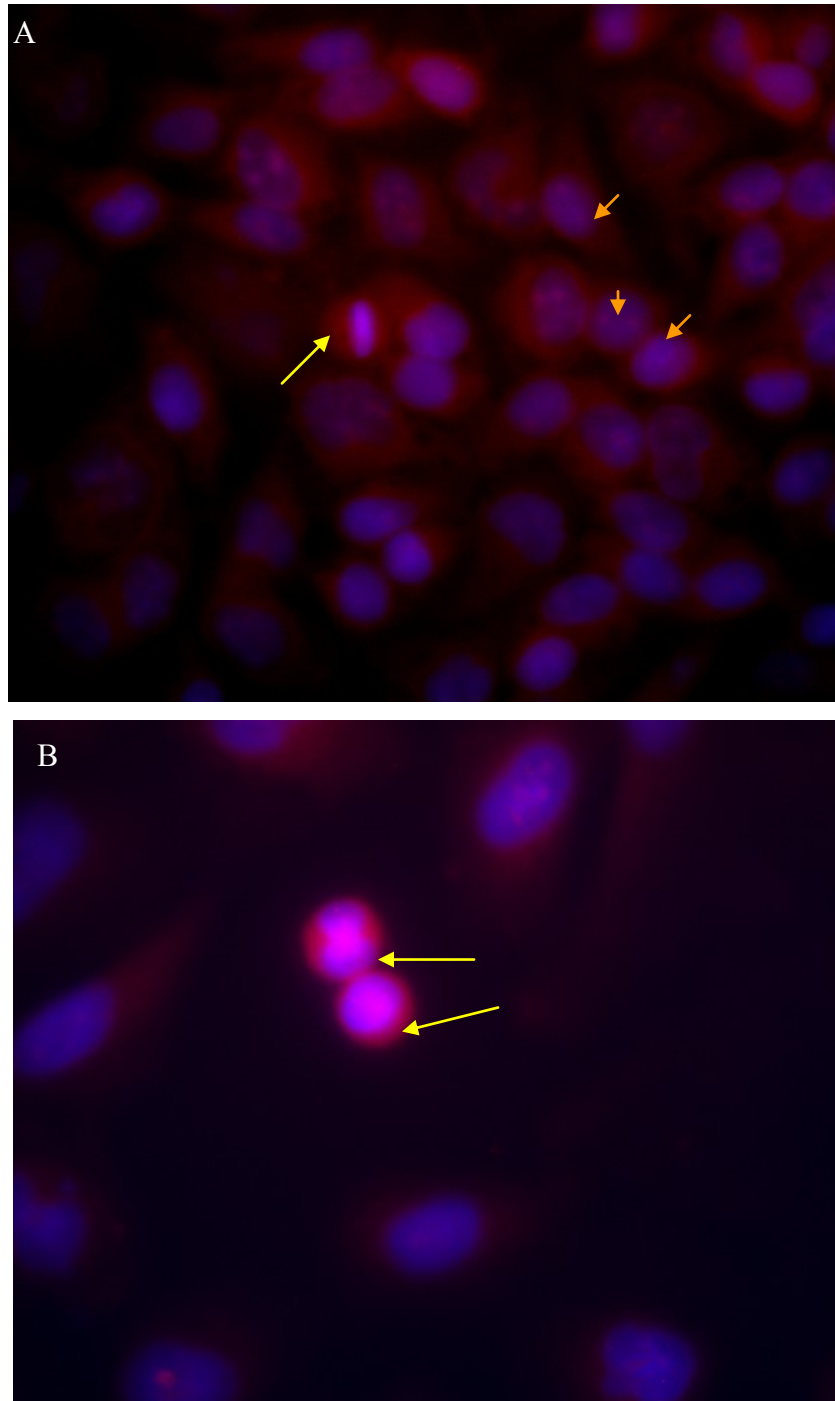


**Figure 4 - Localization of APC subunits in unsynchronized HeLa cells.**

Apc11 (A) and Cdc20 (B) are shown in red. Hoechst 22358 (Chromatin) is shown in blue. Evidence of colocalization is purple.  $G_2$  cells show a cytoplasmic distribution of APC subunits while cells undergoing cellular replication show evidence of colocalization around the chromatin. Orange arrows point to the kinetochores in prophase cells. Yellow arrows point to a cell in metaphase. Red fluorescence is imaged with a 100 ms exposure.

For Cdc20, the localization pattern is very similar (Figure 4B). In non-dividing ( $G_2$ ) cells, dim cytoplasmic and nuclear staining is detected. Once the cells enter mitosis, the anti-Cdc20 is significantly more detectable around the dividing sister chromatids, though not directly on the spindle fibers as in the Apc11 staining (*yellow arrows*). This is also consistent with previous work (Clute & Pines, 1999).

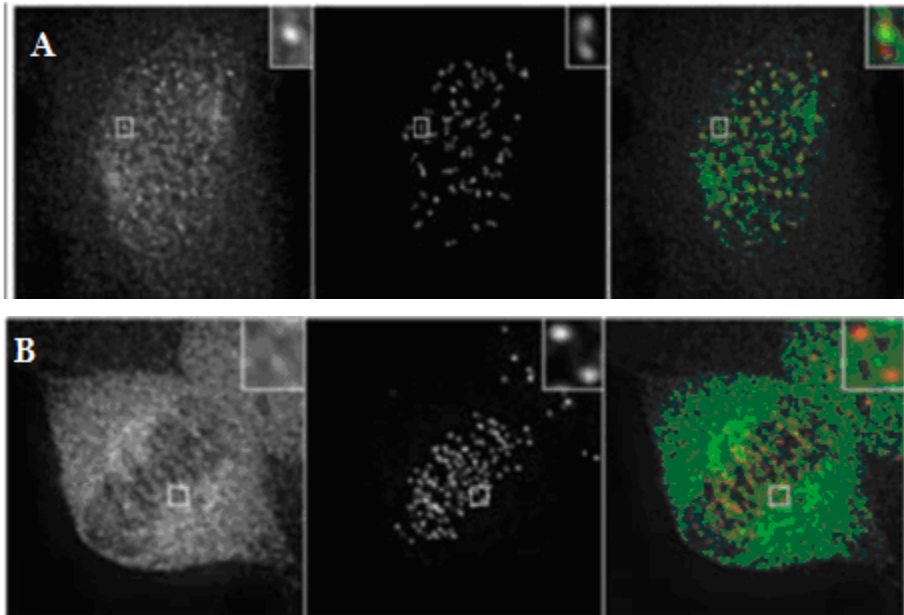


**Figure 5 - Published images of APC3 localization (Acquaviva *et al.* 2004)**

APC3 (left panel, green) was localized in synchronized HeLa cells. CREST staining of centromeres is shown in the middle panels. The right panel is the merge of the two. At prophase (A), APC3 staining is detected at the kinetochores while at metaphase (B), staining is detected at the mitotic spindle.

The anti-Rec8 antibody was also initially validated with HeLa cells. Rec8 has been known to be a highly regulated protein (reviewed by Watanabe *et al.*, 2005). It has been previously demonstrated that, while at metaphase Rec8 is highly associated with the chromosomes, Rec8 is soon cleaved and disperses throughout the cytoplasm. This is similar to the localization pattern seen in Figure 6. HeLa cells were grown on coverglass to 75% confluence and fixed in 2% PFA with Triton X-100. Cells were stained for Rec8 (*red*) and chromatin (*blue*). Non-replicative cells appear show a non-distinct cytoplasmic Rec8 staining. However, the cell at metaphase (*yellow arrow*) shows bright Rec8 staining around the chromosomes.

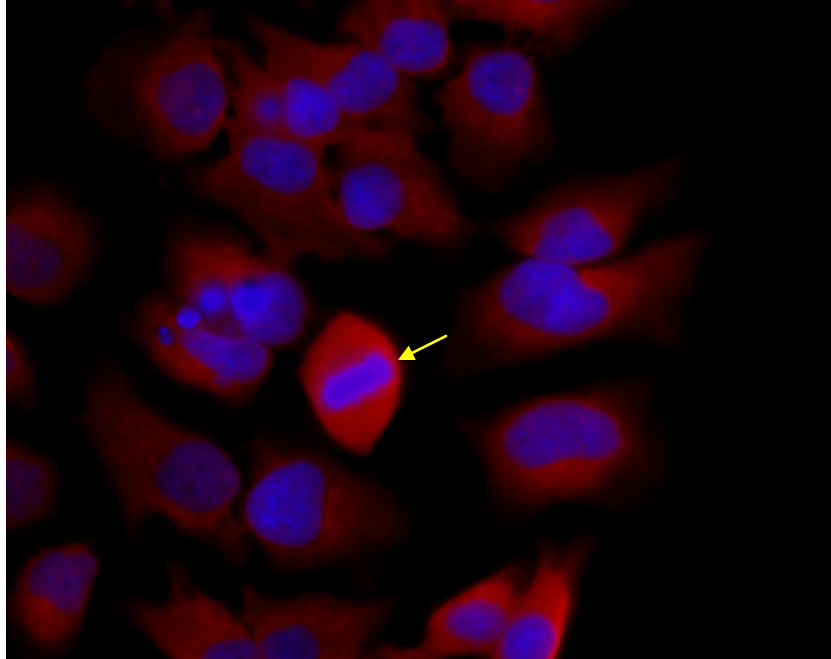


**Figure 6 - Localization of Rec8 in unsynchronized HeLa cells.**

Anti-Rec8 is stained in red. Hoechst 22358 (Chromatin) is stained in blue. At metaphase, Rec8 (*red*) is highly expressed around the chromosomes (*blue*) aligned around the metaphase plate (*yellow arrow*). In non-dividing cells, Rec8 staining is less distinct in the cytoplasm. Red fluorescence is imaged with a 100 ms exposure.

## ***Part II: Optimization***

### **Dilution study**

Once the antibodies were validated, it was then necessary to optimize the staining protocol in a mouse oocyte system. In order to determine the ideal experimental conditions, staining variables such as primary antibody concentration, incubation temperature, and duration all needed to be addressed. In brief, a series of experiments was designed such that primary concentration, incubation time, and temperature were individually varied. A similar process was completed for the optimization of Apc11 (Figure 8), Cdc20 () and Rec8 (*data not shown*). The detailed experimental design is provided in the Methods and Materials section.

Figure 7 shows representative results of negative control experiments. To generate these images, oocytes were subjected to the same staining protocol listed in the Materials and Methods section without the addition of secondary antibody (Figure 7B-D). Figure 7A shows an egg stained with neither primary nor secondary antibodies. In all

oocytes, low levels of non-distinct staining could be detected. It was this base level of fluorescence to which all subsequent images were compared.

The pictures in Figure 8 are representative of the optimization study for Apc11. Oocytes were fixed at metaphase of meiosis II in 2% PFA with Triton X-100. Apc11 appears in green. Chromatin stained with Hoechst 22358 appears blue. Tubulin (meiotic spindle) is stained red. In samples incubated in high concentrations of anti-Apc11 (every dilution tested below 1:1000, *data not shown*), the staining pattern was that of complete saturation. Camera saturation occurs when pixel values exceed the range of the camera and are assigned as white.

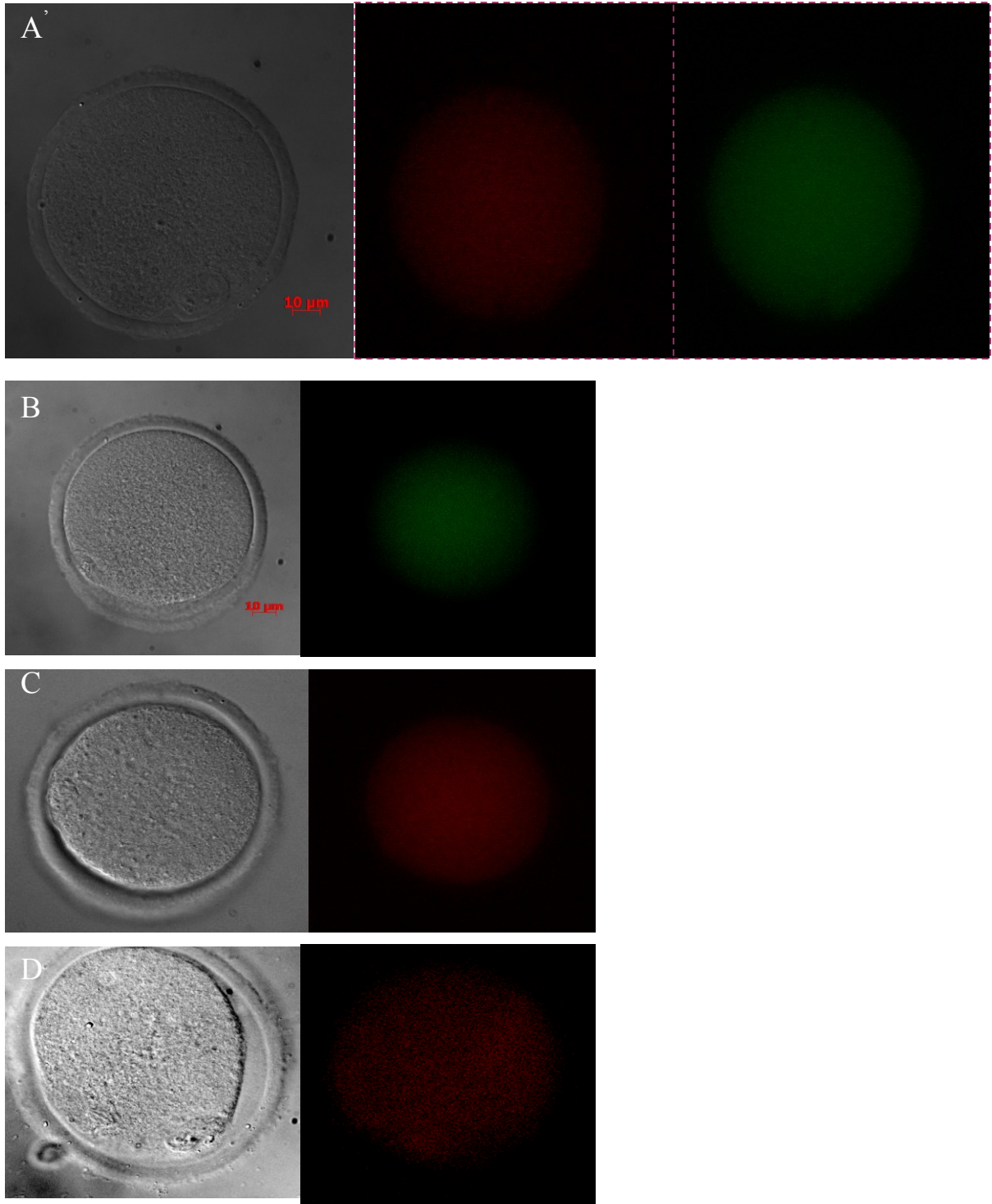


**Figure 7 - Negative control images of oocytes**

Oocytes were imaged without the addition of secondary and/or primary antibodies in the staining protocol: neither primary nor secondary antibody (A), Apc11 alone (B), Cdc20 alone (C), or Rec8 alone(D) without the addition of secondary antibody. DIC images (left) are shown with 5ms exposure; fluorescence images (right) are shown with a 150 ms exposure. The background has been set to black.

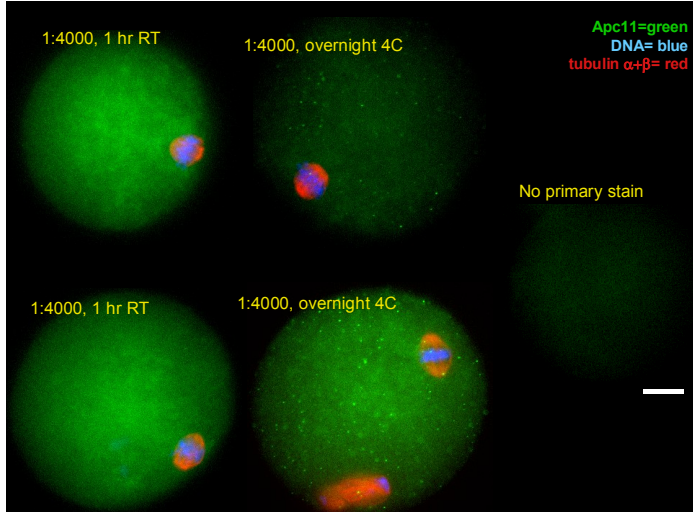
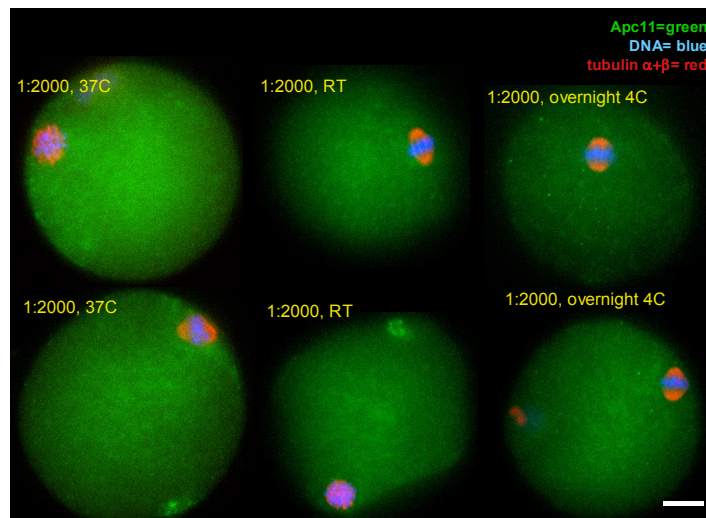
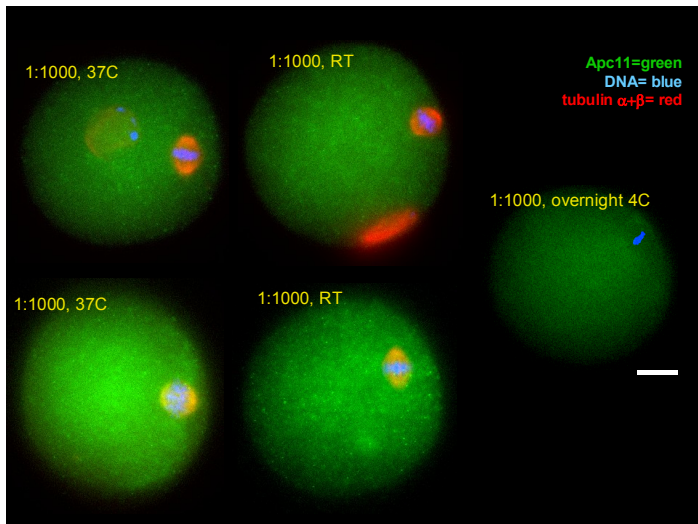


### Figure 8 - Apc11 staining optimization in mouse oocytes.

Oocytes fixed in 2% PFA with Triton X-100 were incubated in decreasing concentrations (1:1000, *top panel*), (1:2000, *middle panel*), (1:4000, *bottom panel*) of Apc11 either overnight at 4°C or for 1 hour at either room temperature or 37°C. Oocytes were stained for Apc11 (green), Hoechst 22358 (blue), tubulin (red). Oocyte autofluorescence appears as a dull green haze. Scale bars are 15µm. All green fluorescence imaged with a 100 ms exposure.

At high concentrations, it was impossible to differentiate any variation in the pattern within a single oocyte or between other oocytes (data not shown). At the 1:1000 dilution (Figure 8 *top panel*), distinct Apc11 localization patterns appeared within the oocyte (cytoplasmic staining, cortical omission, and an exclusion zone within the meiotic spindle, *detailed later*). As the dilution was increased to 1:2000 (Figure 8 *middle panel*), these patterns became more consistently apparent. While these patterns were still detectable in the 1:4000 dilution (Figure 8 *bottom panel*), the staining pattern was often so dim, that it was difficult to discern the antibody from the

background auto-fluorescence of the oocyte (shown in Figure 7). It was therefore determined that a 1:2000 dilution of anti-Apc11 was optimal for the purposes of this project.

For this experimental set, secondary antibody conditions were held constant at 5ug/ml.

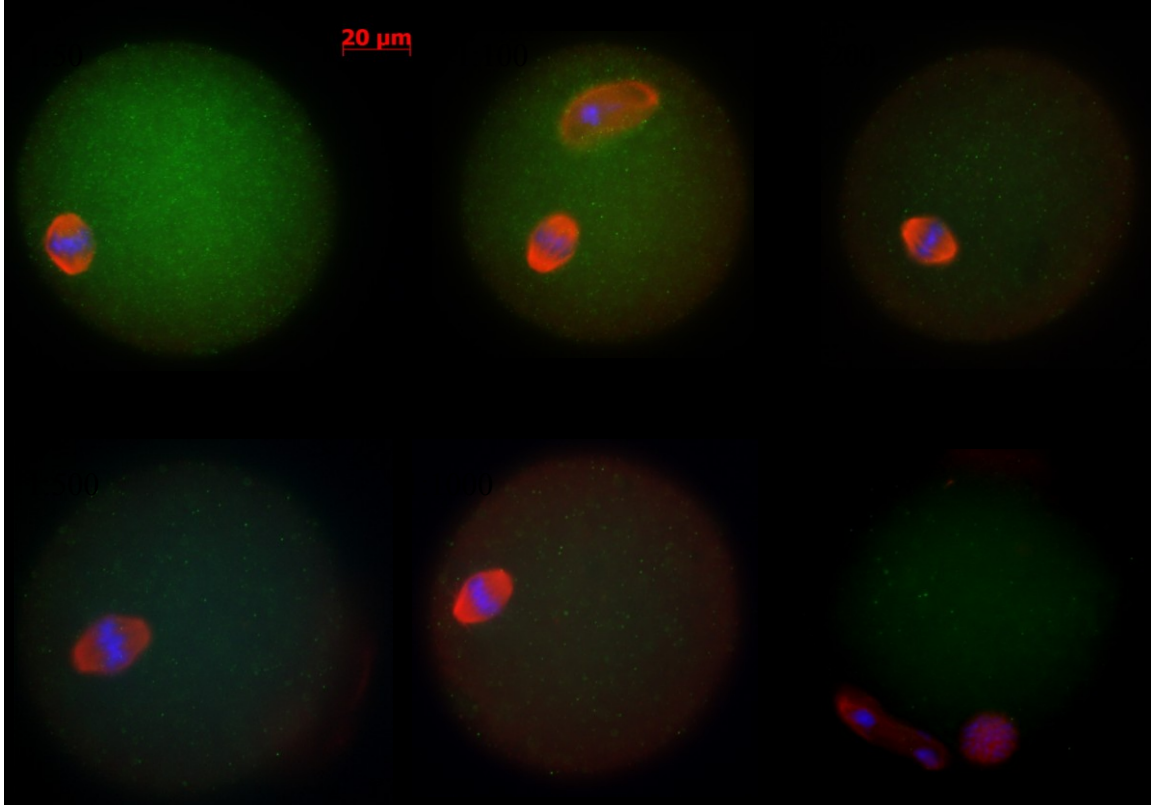


**Figure 9 - Examples of Cdc20 optimization**

Oocytes fixed in 2% PFA with Triton X-100 were incubated in increasing concentrations of primary cdc20 antibody. Oocytes were stained for Cdc20 (green), Hoechst 22358 (blue), tubulin (red). Oocyte autofluorescence appears as a dull green haze. Scale bars are 20μm. All green fluorescence imaged with a 100 ms exposure.

## Incubation temperature and duration

Once a dilution was selected, it was then necessary to determine the optimal conditions for temperature and duration of immunostaining. Oocytes were incubated overnight at 4°C or for one hour at either 37°C or room temperature. While oocytes stained at 37°C yielded bright images (Figure 8 *middle panel-left*), often the signal reported by the camera was saturated and therefore may not have been as specific as the pictures taken of oocytes incubated at lower temperatures. In contrast to this, oocytes incubated for 1 hour at room temperature (Figure 8 *middle panel-middle*), were often too dim to discern any consistent localization. Similarly, oocytes stained at 4°C overnight

(Figure 8 *middle panel-right*) were also fairly dim, but localization within these oocytes appeared more consistent than those stained at room temperature. Because of this, an overnight incubation at 4°C was used for the remainder of the Apc11 studies.

### Fixative comparison

Another factor that has a profound effect on staining specificity and the imaging process is the solution used to fix the oocytes. Ideally, the fixative should preserve the structure of certain aspects of an immobilized cell in order to help predict the utility of those aspects *in vivo*. For example, if conducting studies on the meiotic spindle, a fix

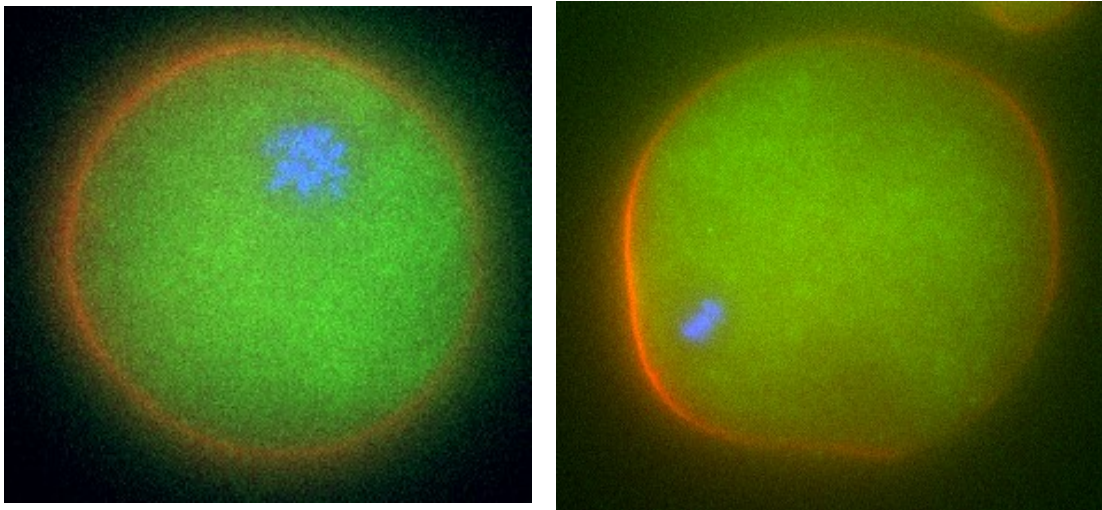


**Figure 10 - Oocytes fixed with MTSB-XF.**

Oocytes were fixed at MII with MTSB-XF and stained with anti-Apc11 (*green*), Hoechst 22358 (*blue*), and Phalloidin labeled with Texas Red (*red*). While Apc11 localization can still be detected in an exclusion zone around the meiotic spindle, the overall staining pattern is non-distinctive.

solution that would preserve the native microtubule structure at a given time while simultaneously removing material that would restrict access to the spindle would be ideal. In the mouse system, one such fix is the Microtubule Stabilizing Buffer - Extraction Fixative (MTSB-XF) used by (Ibanez *et al.*, 2003) who carefully measured the

morphology of the meiotic spindle in response to a variety of stimuli. Since the anaphase promoting complex was known to act in the vicinity of the meiotic spindle, MTSB-XF was chosen as the fix solution for the initial studies of the Apc11 antibody.

Representative results of these initial studies are shown in Figure 10. Oocytes arrested at MII were stained with Anti-Apc11 (*green*), Hoechst 22358 (*blue*), and Texas-red Phalloidin (*red*). Although an Apc11 localization pattern can be detected as an exclusion zone surrounding the meiotic spindle, the overall stain is hazy and non-distinctive. For this reason, MTSB-XF was replaced by the PFA solution described in the Methods and Materials section as the preferred fixative (compare Figure 10 to Figure 11; *detailed later*).

### **Selection of an activation stimulus**

As oocytes develop, they undergo a complete round of meiosis and then arrest at metaphase of meiosis II. Oocytes will remain in this arrested state until they are ionically activated to continue development. Normally, this stimulus is a periodic calcium signal produced by the invading sperm to the oocyte. However, in order to study the spatial localization of the anaphase-promoting complex at different stages of development, this signal was initially replicated *in vitro* with a short incubation in 5% Ethanol. Ethanol causes the formation of inositol 1,4,5-triphosphate at the membrane and a concomitant influx of extra-cellular calcium (Ibanez *et al.*, 2005). However, instead of periodic spikes in cytoplasmic calcium concentration, the ethanol causes a prolonged influx of calcium. As a result, oocytes activated with ethanol developed inconsistently. Often, as many as 50% of eggs per experiment failed to leave MII when activated by a standard ethanol protocol (*data not shown*). Additionally, eggs that did activate often progressed through development too quickly for the cell to properly respond. Since this phenomenon often caused significant egg-to-egg variation in control groups (*data not shown*), ethanol was replaced as an activation stimulus by strontium chloride for all subsequent experiments.

### **Part III. Apc11 Localization**

Demecolcine has been used to aid in the enucleation process for the purposes of somatic cell nuclear transfer (Baguisi & Overstrom, 2000). In order to test the effects of

Demecolcine on the spatial localization of Apc11, the catalytic core of the Anaphase-Promoting Complex, oocytes harvested from hormonally primed CF-1 mice were activated in strontium chloride, incubated in the presence of 0.4ug/ml Demecolcine, and fixed in PFA solution at specific points of development (AII, TII, Interphase). Control eggs were fixed without ever being exposed to Demecolcine. The results of these control experiments can be found in Figure 11 through Figure 14. Anti-Apc11 is shown in green. Chromatin appears blue. Tubulin appears red. Left panels show Apc11 alone; right panels are the overlay of the three stains.

A minimum of 10 eggs were imaged for every treatment with each antibody. Unless otherwise stated, all images presented were representative of the treatment group with little egg to egg variation.

## Control activation

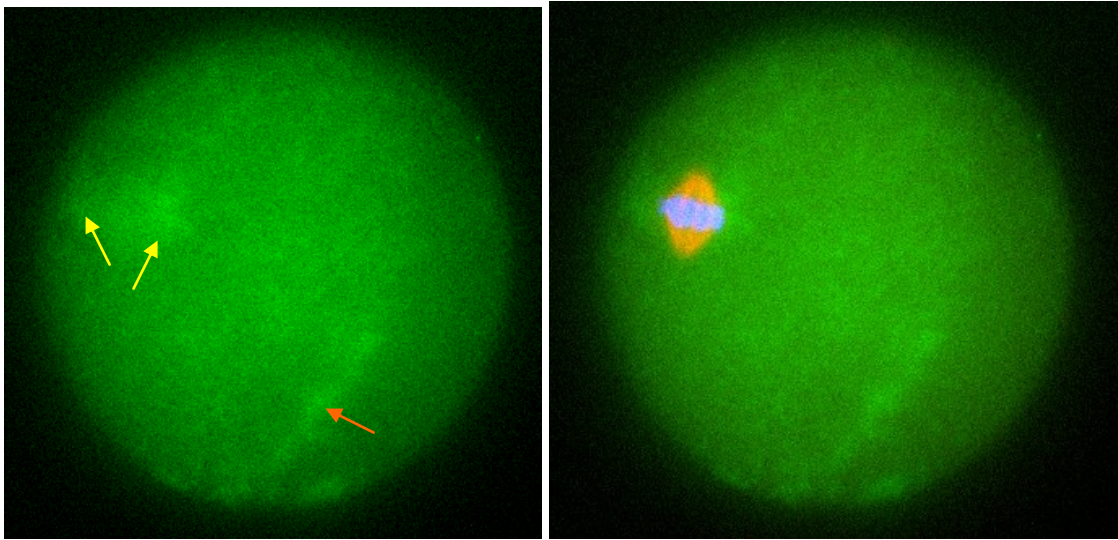


**Figure 11 - Localization of Apc11 in oocytes arrested at Metaphase of meiosis II (MII).** Denuded oocytes were fixed in PFA immediately following removal from hyaluronidase and stained for Apc11 (*green*), chromatin (*blue*), and  $\alpha+\beta$  tubulin (*red*). The left panel shows Apc11 alone; the right panel is the overlay of the three stains. Yellow arrows indicate perispindular localization. Orange arrow indicates the hemispheric ridge. Green fluorescence is imaged at 120ms.

During meiosis II, Apc11 (*green*) showed two types of localization. The most prevalent was a strong localization to the area directly surrounding the meiotic spindle (Figure 11, *yellow arrows*). This perispindular localization persisted from MII (Figure 11), through AII (Figure 12) and TII (Figure 13) and began to disappear at the onset of interphase (Figure 14). Interestingly, while there existed a high concentration of Apc11 outside the spindle, there was very little staining in the area directly within the spindle (*not shown in the focal plane of Figure 11; see Figure 13*). This staining continued to surround the chromatin (though less pronouncedly) even after the spindle has moved away at Interphase (Figure 14). The second type of localization occurred only at MII and early AII. Within these oocytes, there appeared to be a discrete staining pattern within the hemisphere that contained the meiotic spindle (Figure 11, *orange arrow*).

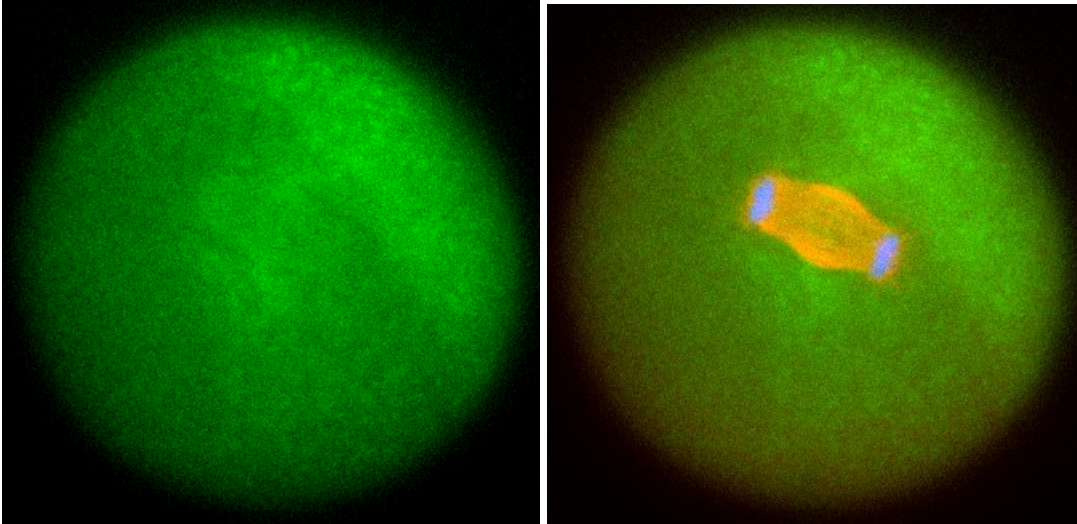


**Figure 12 - Localization of Apc11 in oocytes fixed at Anaphase of meiosis II (AII).** Denuded oocytes were fixed in PFA 25 minutes after the initiation of activation. Oocytes were stained for Apc11 (*green*), chromatin (*blue*), and  $\alpha+\beta$  tubulin (*red*). The left panel shows Apc11 alone; the right panel is the overlay of the three stains. Green fluorescence is imaged at 120ms.

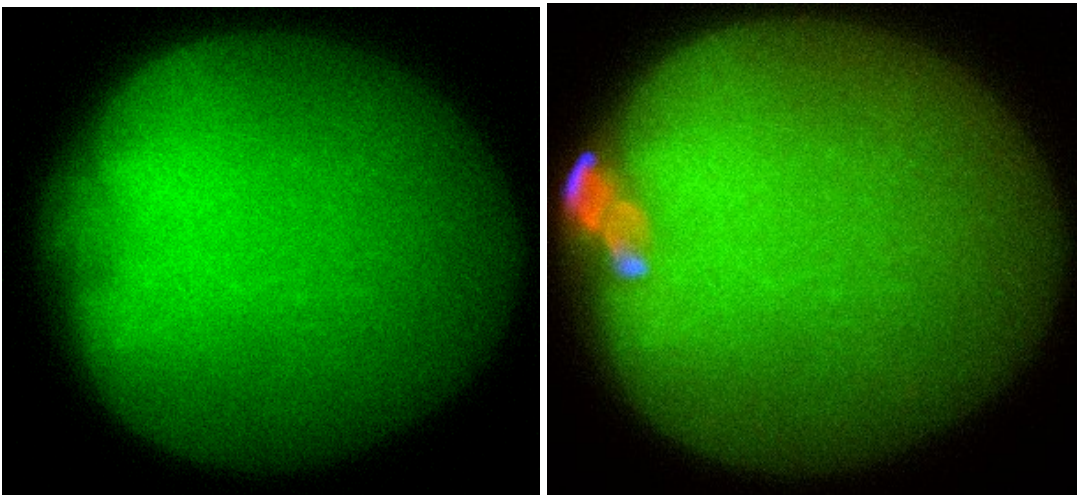


**Figure 13 - Localization of Apc11 in oocytes fixed at Telophase of meiosis II (TII).** Denuded oocytes were fixed in PFA 2 hours after the initiation of activation. Oocytes were stained for Apc11 (*green*), chromatin (*blue*), and  $\alpha+\beta$  tubulin (*red*). The left panel shows Apc11 alone; the right panel is the overlay of the three stains. Green fluorescence is imaged at 120ms.

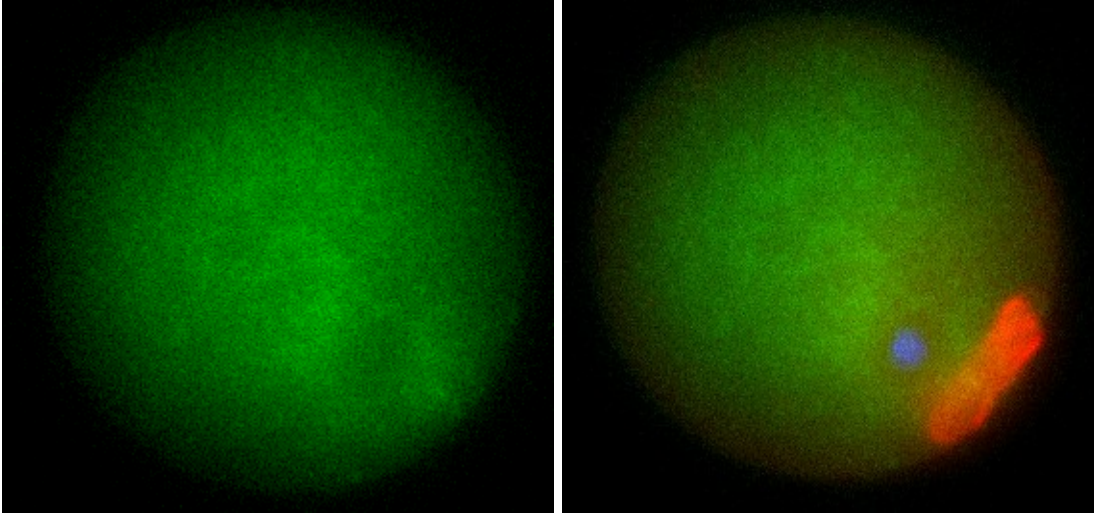


**Figure 14 - Localization of Apc11 in oocytes fixed in Interphase.**

Denuded oocytes were fixed in PFA 4 hours after the initiation of activation. Oocytes were stained for Apc11 (*green*), chromatin (*blue*), and  $\alpha+\beta$  tubulin (*red*). The left panel shows Apc11 alone; the right panel is the overlay of the three stains. Green fluorescence is imaged at 120ms.

### **Effects of Demecolcine on Apc11 spatial localization**

Once the spatial localization of Apc11 following a standard parthenogenetic activation was established, it was then possible to determine what effects Demecolcine may have on its localization. Oocytes were incubated 10 minutes in strontium chloride before they were transferred into media containing both strontium chloride and Demecolcine (0.4ug/ml). The results of these experiments can be found in Figure 15 through Figure 17. Anti-Apc11 is shown in green. Chromatin appears blue. Tubulin appears red. Left panels show Apc11 alone; right panels are the overlay of the three stains.

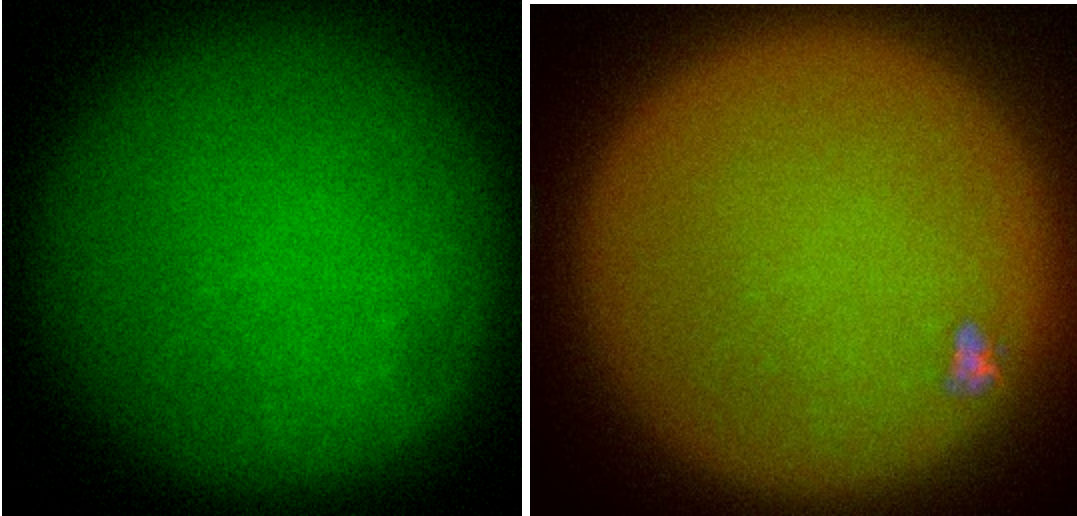


**Figure 15 - Effects of Demecolcine on Apc11 localization in oocytes fixed at AII.**

Denuded oocytes were incubated in 10mM SrCl<sub>2</sub> for 10 minutes followed by a 15 minute incubation in media containing 10mM SrCl<sub>2</sub> and 0.4ug/ml Demecolcine. (*left panel*) Apc11 alone. (*right panel*) Overlay of Apc11 (*green*), Hoechst 22358 (*blue*), and  $\alpha+\beta$  tubulin (*red*). Green fluorescence is imaged at 120ms.

As seen in Figure 15, the Demecolcine destabilized the microtubules within the cell. As a result, the meiotic spindle was severely disrupted compared to control eggs at the same time (see Figure 12) and tubulin (*red staining*) was detected throughout the cytoplasm. Furthermore, a longer incubation in Demecolcine caused more of the microtubules to disassociate from the spindle (compare red staining in Figure 15 to Figure 17). Because the spindle was disrupted, sister chromatids often did not segregate properly and only a single cluster of DNA was observed well after the activation stimulus. Eventually, the oocyte completely extrudes its chromatin in the second polar body (Figure 17).

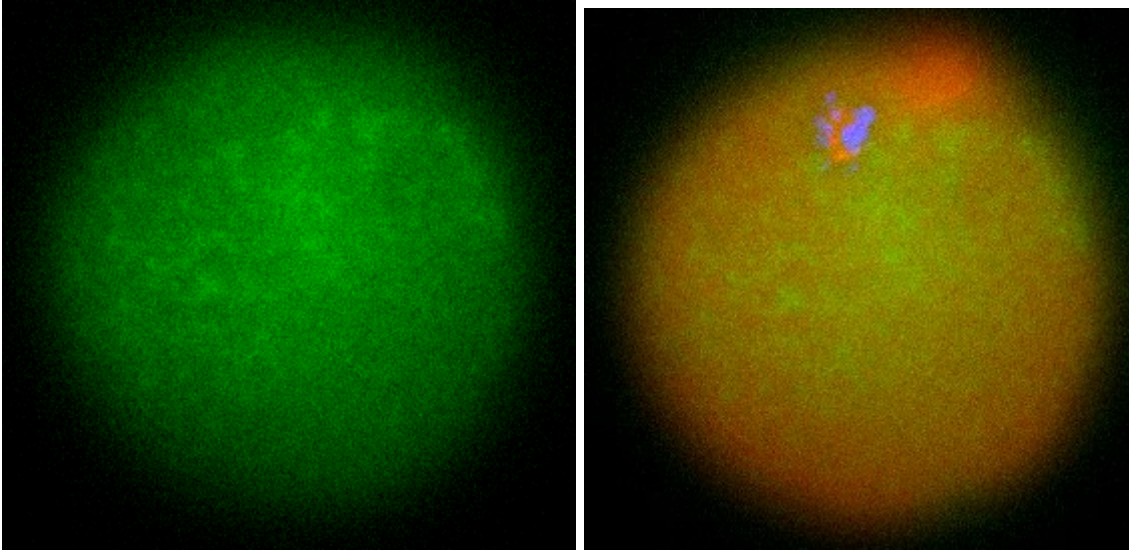


**Figure 16 - Effects of Demecolcine on Apc11 localization in oocytes fixed at TII.** Denuded oocytes were incubated in 10mM SrCl<sub>2</sub> for 10 minutes followed by a 110 minute incubation in media containing 10mM SrCl<sub>2</sub> and 0.4ug/ml Demecolcine. (*left panel*) Apc11 alone. (*right panel*) Overlay of Apc11 (*green*), Hoechst 22358 (*blue*), and  $\alpha+\beta$  tubulin (*red*). Green fluorescence is imaged at 120ms.

Since the spatial localization of many key cell cycle proteins is closely associated to the meiotic spindle, it was hypothesized that the disruption of that spindle could negatively affect subunits of the APC as well. As Figure 15 through Figure 17 show, the disruption of the meiotic spindle did cause a concomitant loss of Apc11 localization. Apc11 localization in mouse eggs is characterized by an aggregation of protein directly around the spindle. However, in eggs treated with Demecolcine, the staining pattern changed to a non-distinct ataxia across the entire oocyte with no evidence of colocalization in any stage of development.

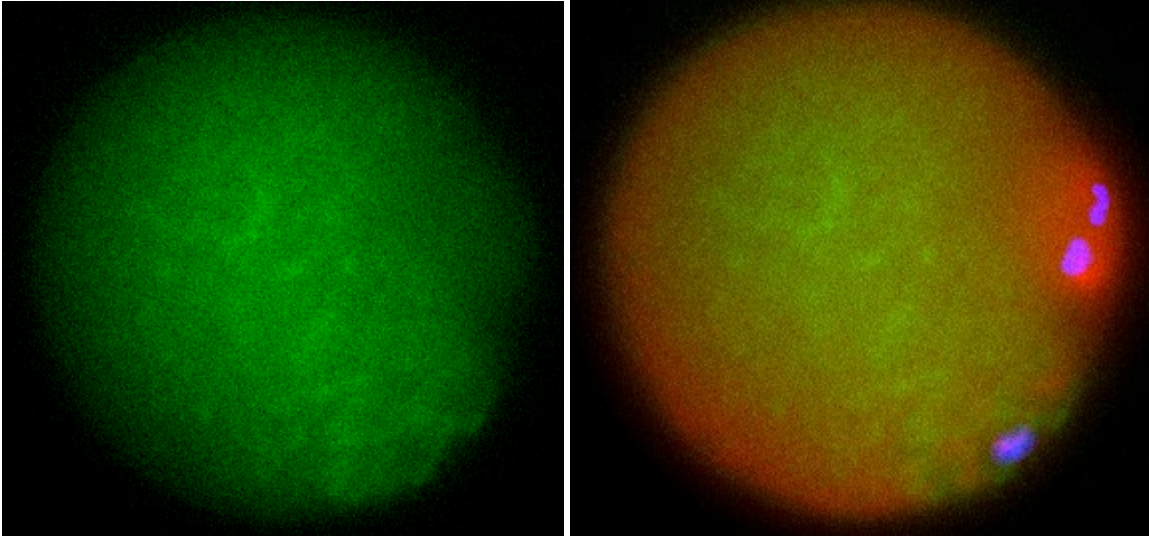


**Figure 17 - Effects of Demecolcine on Apc11 localization in oocytes fixed at Interphase.** Denuded oocytes were incubated in 10mM SrCl<sub>2</sub> for 10 minutes followed by a 230 minute incubation in media containing 10mM SrCl<sub>2</sub> and 0.4ug/ml Demecolcine. (*left panel*) Apc11 alone. (*right panel*) Overlay of Apc11 (*green*), Hoechst 22358 (*blue*), and  $\alpha$ + $\beta$  tubulin (*red*). Green fluorescence is imaged at 120ms.

## **Part IV. Cdc20 Localization**

In the regulation of development, Cdc20 has the dual role of both an activator of the Anaphase Promoting Complex and a substrate of the ubiquitin-assisted destruction pathway. During metaphase of mitosis, Cdc20 binds to the APC allowing for the ubiquitination of securin. Once the cell progresses beyond early anaphase, Cdc20 disassociates from the complex and is soon destroyed. In order to determine if this pattern in mitosis correlates to meiotic cells, Cdc20 was localized in mouse eggs with a commercially available polyclonal antibody.

### **Control activation**

Oocytes were harvested from the oviducts of hormonally primed CF-1 mice and separated from the surrounding cumulus mass with bovine hyaluronidase (HA). Denuded oocytes were either fixed immediately at metaphase of meiosis II or activated with 10mM strontium chloride and fixed later in development in 2% PFA with Triton X-100 (AII, TII, Interphase). Oocytes were stained for Cdc20 (*red*), chromatin (*blue*), and  $\alpha+\beta$  tubulin (*green*).

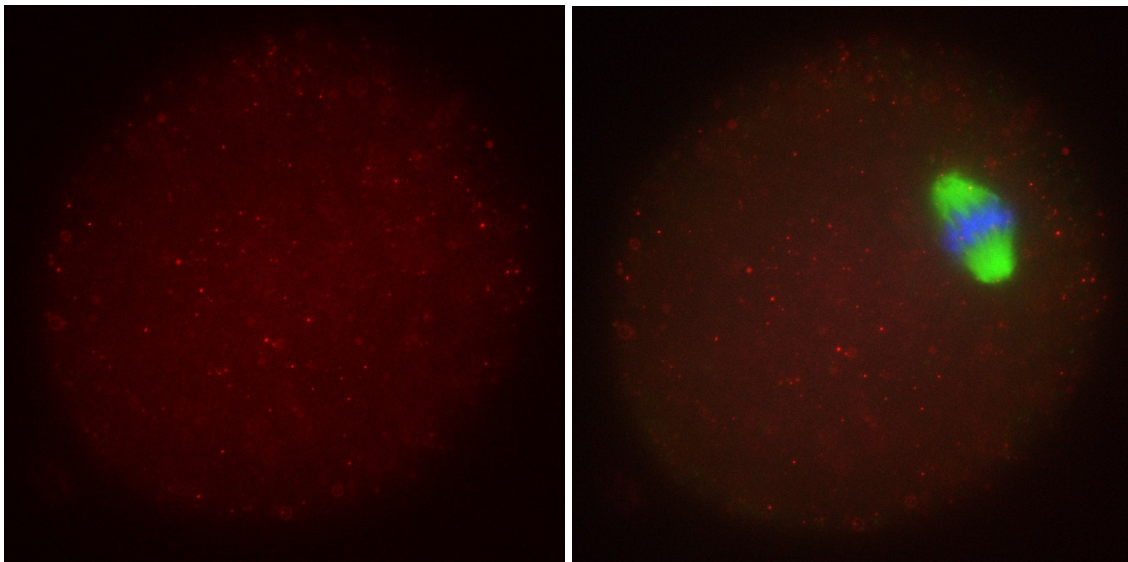


**Figure 18 - Localization of Cdc20 in oocytes fixed at MII.**

Denuded oocytes were fixed immediately following removal from hyaluronidase. (*left panel*) Cdc20 alone. (*right panel*) Overlay of Cdc20 (*red*), Hoechst 22358 (*blue*), and  $\alpha+\beta$  tubulin (*green*). At MII, Cdc20 stained shows punctate spots throughout the cytoplasm. Red fluorescence is imaged at 100ms.

At MII, Cdc20 staining (*red*) appeared as punctate spots seemingly randomly distributed throughout the cytoplasm. Therefore, unlike Apc11, Cdc20 did not appear to localize to the vicinity of the meiotic spindle in metaphase. This variegate staining disappeared early after activation. At AII, the staining pattern changed to a more diffuse cytoplasmic distribution across the cell (*see* Figure 19). By TII (Figure 20), Cdc20 staining has all but disappeared, with only a faint haze remaining across the cytoplasm. This miasma is indistinguishable from the natural autofluorescence of oocytes fixed with PFA (*data not shown*). Interestingly, Cdc20 staining reappears in oocytes fixed in Interphase (Figure 21). At this point in development, Cdc20 localizes strongly to the pronucleus (*yellow arrow*) and diffusely to the cytoplasm. This cytoplasmic staining is comparable to the staining observed at AII (compare Figure 21 to Figure 19).

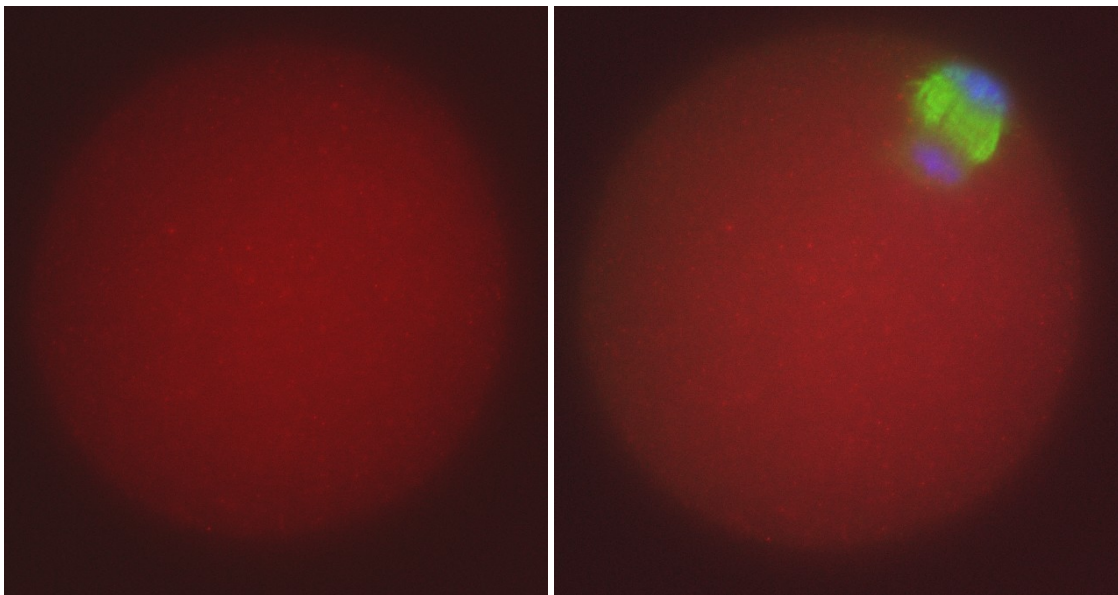


**Figure 19 - Localization of Cdc20 in oocytes fixed at AII.**

Denuded oocytes were fixed after a 25 minute incubation in 10mM SrCl<sub>2</sub>. (*left panel*) Cdc20 alone. (*right panel*) Overlay of Cdc20 (*red*), Hoechst 22358 (*blue*), and  $\alpha+\beta$  tubulin (*green*). At AII, Cdc20 staining shows diffuse cytoplasmic localization. Red fluorescence is imaged at 150ms.

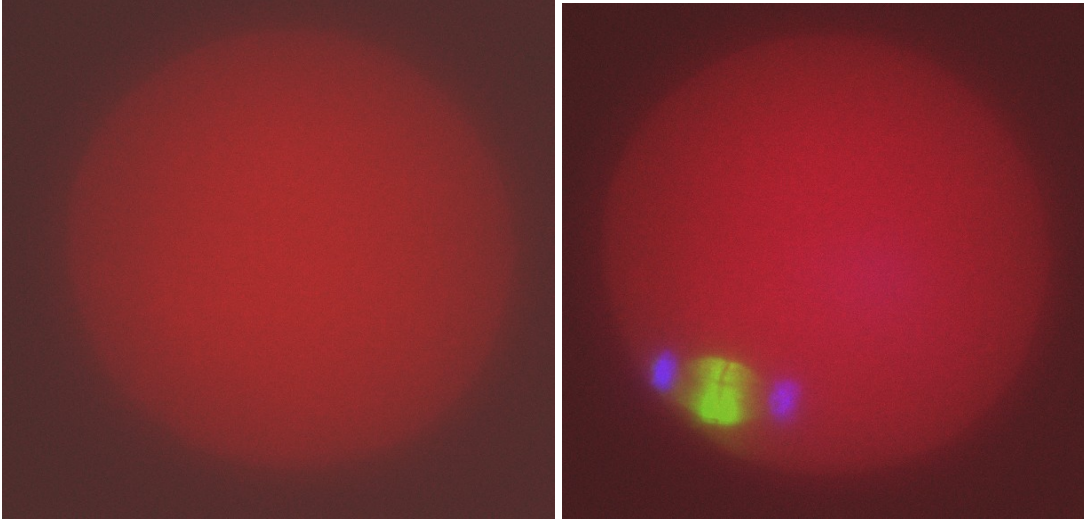


**Figure 20 - Localization of Cdc20 in oocytes fixed at TII.**

Denuded oocytes were fixed after a 1 hour incubation in 10mM SrCl<sub>2</sub>. (*left panel*) Cdc20 alone. (*right panel*) Overlay of Cdc20 (*red*), Hoechst 22358 (*blue*), and  $\alpha+\beta$  tubulin (*green*). At TII, Cdc20 staining shows a dim cytoplasmic haze not significantly brighter than background autofluorescence (*data not shown*). Red fluorescence is imaged at 250ms.

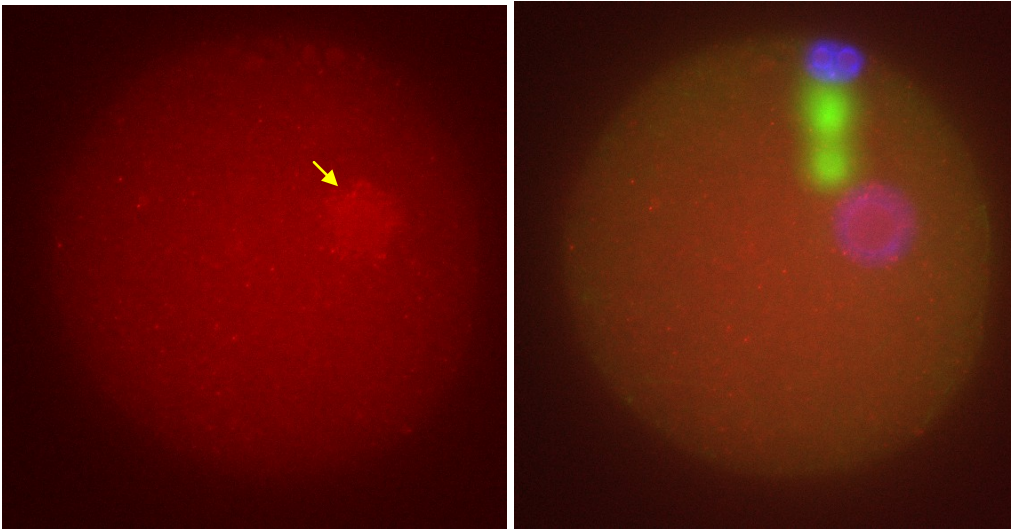


**Figure 21 - Localization of Cdc20 in oocytes fixed at Interphase.**

Denuded oocytes were fixed after a 4 hour incubation in 10mM SrCl<sub>2</sub>. (*left panel*) Cdc20 alone. (*right panel*) Overlay of Cdc20 (*red*), Hoechst 22358 (*blue*), and  $\alpha+\beta$  tubulin (*green*). Red fluorescence is imaged at 150ms.

## Effects of Demecolcine on Cdc20 localization

In order to determine if the localization of Cdc20 is affected by an incubation in Demecolcine, oocytes harvested from hormonally primed CF-1 mice were fixed at

various stages of development in the presence or absence of Demecolcine and stained for Cdc20 (*red*),  $\alpha+\beta$  tubulin (*green*), chromatin (*blue*).

Similar to observations with Apc11, the Demecolcine caused a severely disrupted spindle and the associated cytoplasmic distribution of tubulin and, as the Demecolcine incubation duration was increased, these effects became more prevalent. Also, just as Apc11 was not localized after Demecolcine incubation, so too was Cdc20 affected. While in control eggs, Cdc20 staining levels varied greatly throughout development, nearly disappearing during TII (compare the exposure times of Figure 18 through Figure 21), no such diminution was detected in eggs treated with Demecolcine. As seen in Figure 22, eggs incubated with Demecolcine showed low levels of patchy aggregate staining across the cytoplasm. This pattern persisted throughout development. Thus, the incubation in Demecolcine eliminated the cyclic staining pattern observed in control eggs.

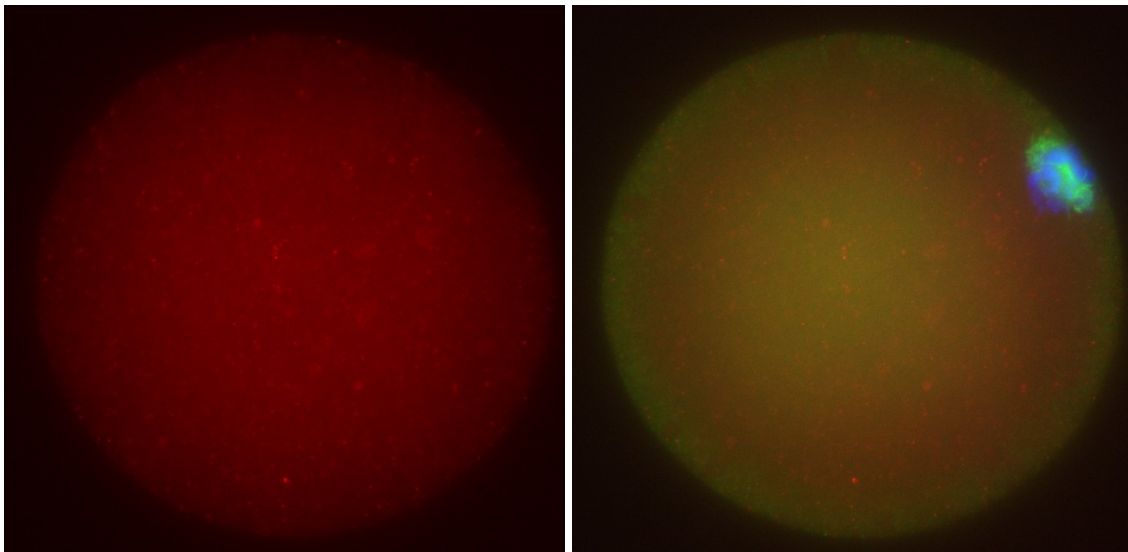


**Figure 22 - Effects of Demecolcine on Cdc20 localization in oocytes fixed at AII.**

Denuded oocytes were incubated in 10mM SrCl<sub>2</sub> for 10 minutes followed by a 15 minute incubation in media containing 10mM SrCl<sub>2</sub> and 0.4ug/ml Demecolcine. (*left panel*) Cdc20 alone. (*right panel*) Overlay of Cdc20 (*red*), Hoechst 22358 (*blue*), and  $\alpha+\beta$  tubulin (*green*). Red fluorescence is imaged at 100ms.

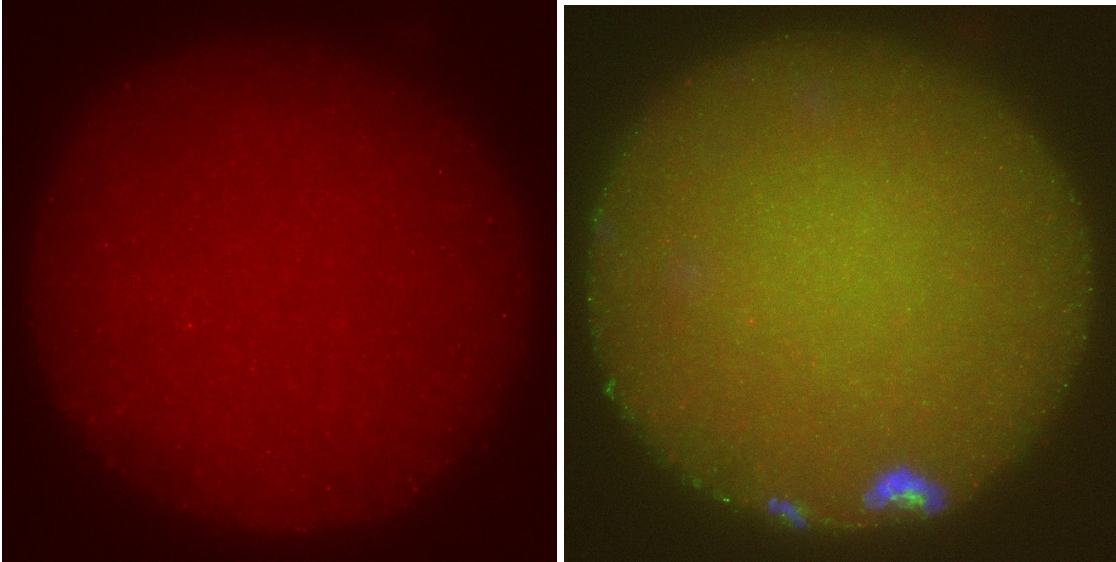


**Figure 23 - Effects of Demecolcine on Cdc20 localization in oocytes fixed at TII.**  
 Denuded oocytes were incubated in 10mM SrCl<sub>2</sub> for 10 minutes followed by a 110 minute incubation in media containing 10mM SrCl<sub>2</sub> and 0.4ug/ml Demecolcine. (*left panel*) Cdc20 alone. (*right panel*) Overlay of Cdc20 (*red*), Hoechst 22358 (*blue*), and  $\alpha+\beta$  tubulin (*green*). Red fluorescence is imaged at 100ms.

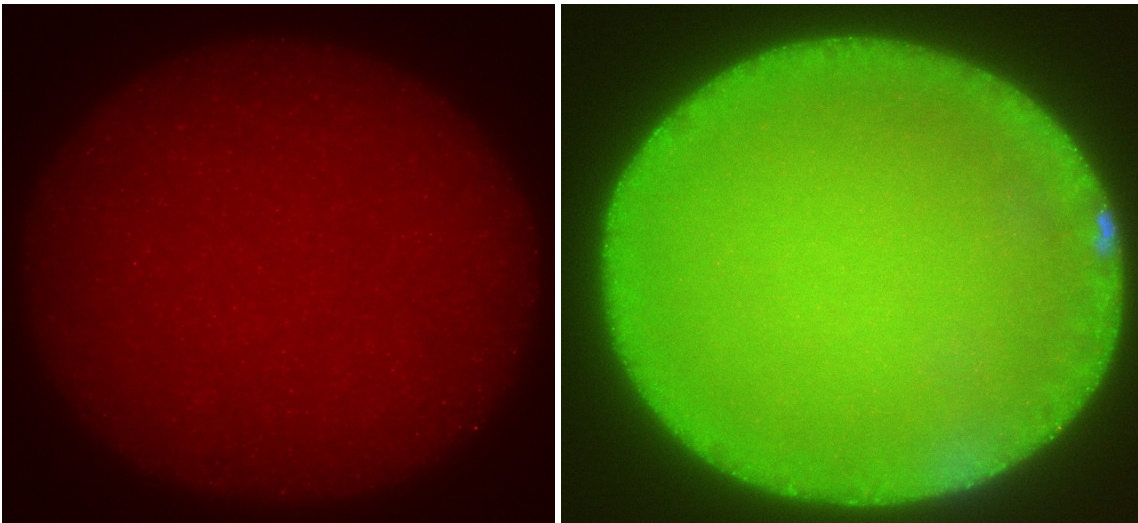


**Figure 24 - Effects of Demecolcine on Cdc20 localization in oocytes fixed at Interphase.**  
 Denuded oocytes were incubated in 10mM SrCl<sub>2</sub> for 10 minutes followed by a 230 minute incubation in media containing 10mM SrCl<sub>2</sub> and 0.4ug/ml Demecolcine. (*left panel*) Cdc20 alone. (*right panel*) Overlay of Cdc20 (*red*), Hoechst 22358 (*blue*), and  $\alpha+\beta$  tubulin (*green*). Red fluorescence is imaged at 100ms.

## ***Part V: Rec8 Localization***

With the knowledge that Demecolcine can affect both the spatial localization of Apc11, the catalytic core of the Anaphase-Promoting Complex, and the orderly destruction of Cdc20, a main activator of the APC, one can postulate that the activity of the APC could also be affected by an incubation in Demecolcine. In order to determine the magnitude of such an effect, the spatial localization of Rec8 was examined.

Rec8 is a meiosis specific subunit of the cohesion complex. In order for a cell to leave metaphase, the APC driven disassembling of the cohesion complex surrounding sister chromatids must occur. The APC, activated by Cdc20, ubiquitinates securin marking it for destruction by the 26S proteasome. The destruction of securin activates separate to open the cohesion complex by the cleavage of the subunit Rec8. Therefore, the spatial localization of Rec8 in relation to cellular chromatin could potentially serve as an indirect measure of downstream APC activity.

### **Control activation experiments**

Since Rec8 localization has not been well characterized in mouse oocytes, it was first necessary to determine the staining pattern in oocytes fixed and activated with a standard parthenogenetic protocol. Denuded oocytes were harvested from hormonally primed CF-1 mice and fixed in 2% PFA with Triton X-100 either immediately after removal from hyaluronidase or activated with 10mM strontium chloride and fixed later in development. They were then stained for chromatin (*blue*) with Hoechst 22358 and Rec8 (*red*) with a commercially available Donkey anti-goat polyclonal antibody (Santa Cruz Biotechnologies).

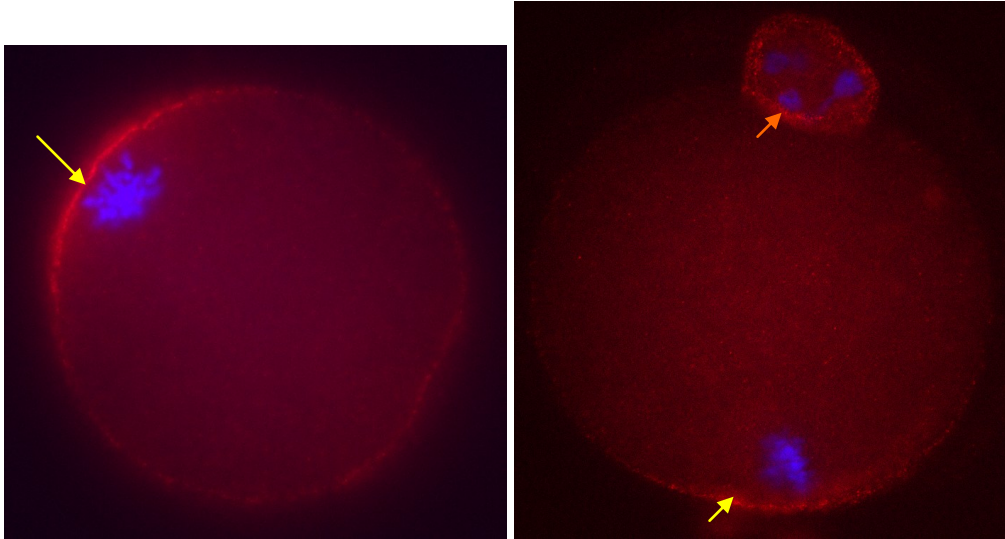


**Figure 25 - Spatial localization of Rec8 in oocytes arrested at MII.**

Denuded oocytes were fixed immediately following removal from hyaluronidase. Overlays of Rec8 (*red*) and Hoechst 22358 (*blue*). At MII, Rec8 localizes to the cortical region directly overlying the condensed chromatin in both the meiotic spindle (*yellow arrows*) and first polar body (*orange arrow*). Red fluorescence is imaged at 120ms.

Anti-Rec8 staining appears to localize to the vicinity of cellular chromatin in several ways. Firstly, Rec8 localizes to the membrane surrounding the first polar body (Figure 25; *right panel, orange arrow* and Figure 26; *bottom panel, aqua circle*). This staining can be seen in all oocytes in which the polar body contains distinguishable chromatin. However, in oocytes where the chromatin within the polar body has begun to deteriorate, there is no evidence of Rec8 polar body localization (*data not shown*).

Secondly, during MII, Rec8 is sequestered to the cortical region directly overlying the metaphase plate (Figure 25; *yellow arrows*). As the sister chromatids begin to separate early in AII, this cortical staining splits as well (Figure 26; *top panel*) remaining closely tied to both sets of chromosomes. As anaphase progresses into telophase (Figure 26; *middle and bottom panels*), it becomes apparent that Rec8 localizes to both the female pronucleus and the budding second polar body. This localization continues through Telophase II (Figure 27) until Interphase when Rec8 becomes partially sequestered within the pronucleus (Figure 28; *yellow arrow*).

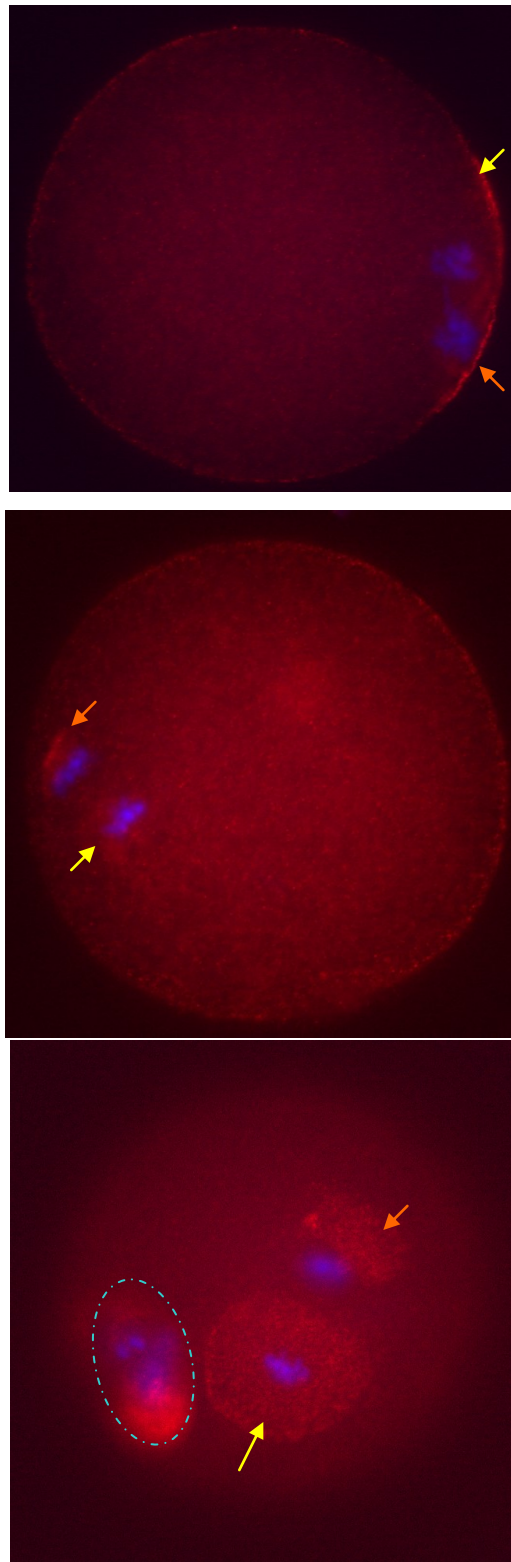


**Figure 26 - Spatial localization of Rec8 in oocytes fixed at AII.**

Denuded oocytes were fixed after a 10 minute (*top panel*), 20 minute (*middle panel*), and a 40 minute (*bottom panel*) incubation in 10mM SrCl<sub>2</sub>. Overlays of Rec8 (*red*) and Hoechst 22358 (*blue*). During anaphase II, Rec8 localizes to an area surrounding chromatin that will become the female pronucleus (*yellow arrows*) and the chromatin that is to be extruded in the second polar body (*orange arrows*). The first polar body is highlighted with an aqua dashed circle. Red fluorescence is imaged at 120ms.

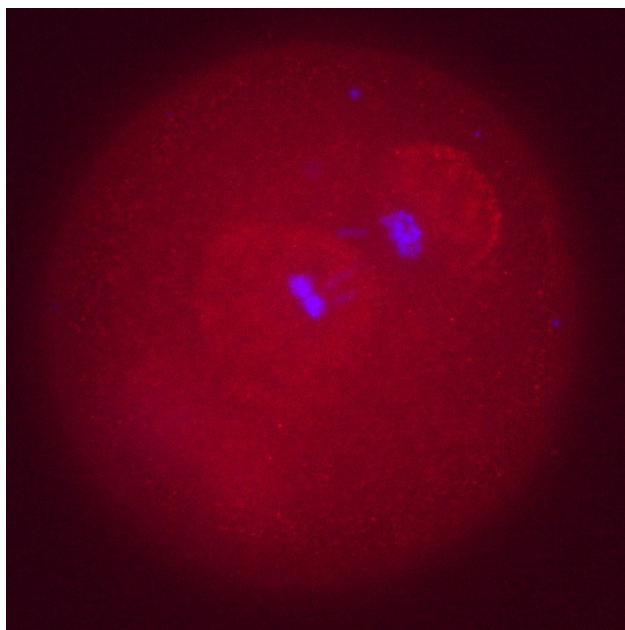


**Figure 27 - Spatial localization of Rec8 in oocytes fixed at TII.**

Denuded oocytes were fix in PFA after a 2 hour incubation in 10mM SrCl<sub>2</sub>. Rec8 is shown in red. Chromatin (Hoechst 22358) is shown in blue. In TII eggs, Rec8 localized around the female pronucleus and the budding second polar body (*similar to the late anaphase oocyte in Figure 26.*) Red fluorescence is imaged at 120ms.

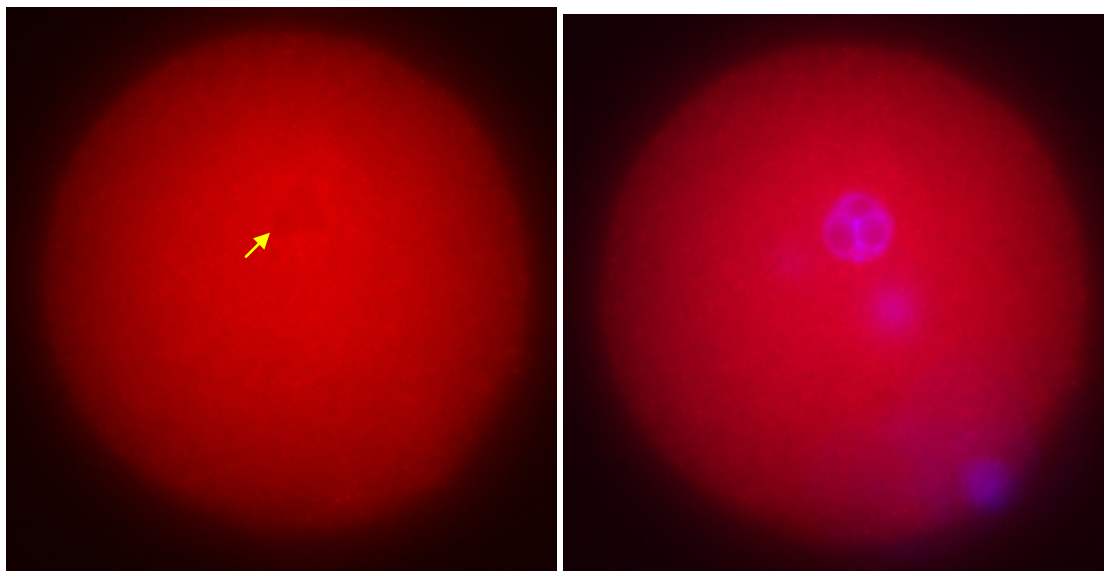


**Figure 28 - Spatial localization of Rec8 in oocytes fixed at Interphase.**

Denuded oocytes were fixed after a 4 hour incubation in 10mM SrCl<sub>2</sub>. Rec8 alone (*left panel*). Overlay of Rec8 (*red*) and Hoechst 22358 (*blue*) (*right panel*). During interphase, some Rec8 remains localized to the female pronucleus (*yellow arrow*) whereas some disperses throughout the cytoplasm. Red fluorescence is imaged at 200ms.

## The effects of Demecolcine on Rec8 localization

Incubation in Demecolcine affected Rec8 localization within mouse oocytes. During anaphase, when the Rec8 normally demonstrated cortical staining directly above the chromatin, Rec8 appeared to aggregate in an area surrounding the chromatin, but not directly over it (Figure 29). Later in development, the Rec8 staining pattern changed. Interestingly, during telophase, Rec8 staining moved from an area near the chromatin to direct colocalization (*purple spots*) with the chromatin (Figure 30; *yellow arrows*). This direct localization continued into interphase as the cell extruded its chromatin in the second polar body (see Figure 31).

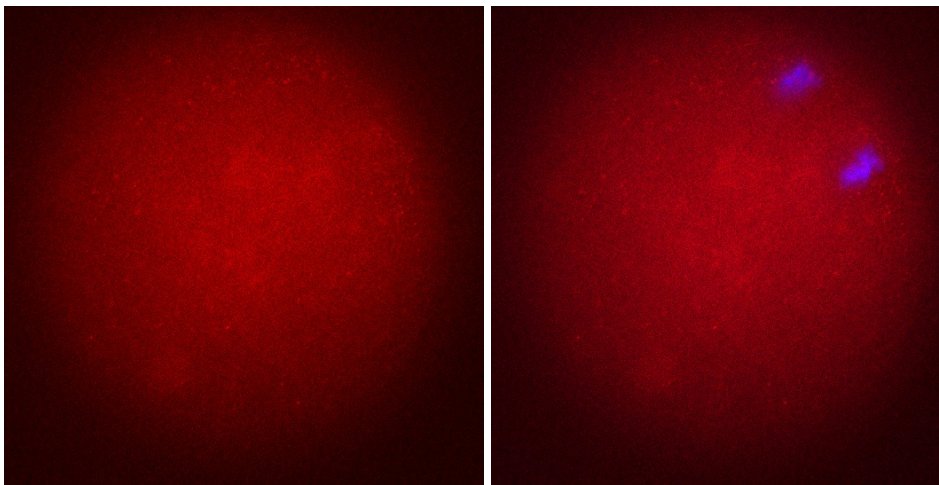


**Figure 29 - The effect of Demecolcine on Rec8 localization in oocytes fixed at AII.** Oocytes were incubated for 10 minutes in 10mM SrCl<sub>2</sub> followed by a 10 minute incubation in media containing both SrCl<sub>2</sub> and 0.4ug/ml Demecolcine before being fixed at AII. Rec8 alone (*left panel*). Overlay of Rec8 (*red*) and Hoechst 22358 (*blue*) (*right panel*). Note the localization of Rec8 near the chromatin but not directly on it. Red fluorescence is imaged at 120ms.

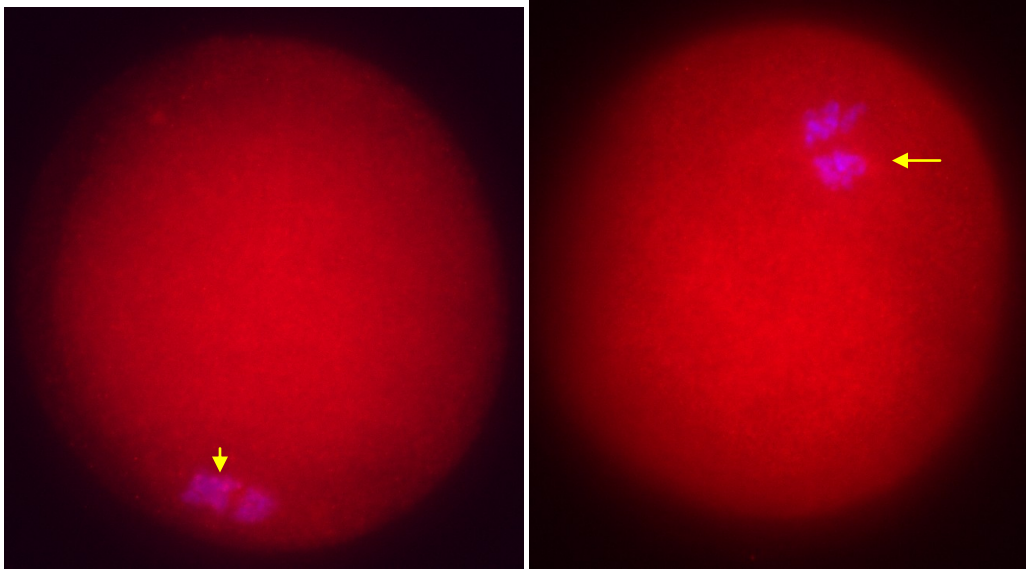


**Figure 30 - The effect of Demecolcine on Rec8 localization in TII eggs.**

Oocytes were incubated for 10 minutes in 10mM SrCl<sub>2</sub> followed by a 70 minute incubation in media containing both SrCl<sub>2</sub> and 0.4ug/ml Demecolcine before being fixed at TII. Overlays of Rec8 (*red*) and Hoechst 22358 (*blue*). In TII eggs treated with Demecolcine, Rec8 colocalizes (*yellow arrows*) directly with chromatin (not the surrounding area). Red fluorescence is imaged at 150ms.

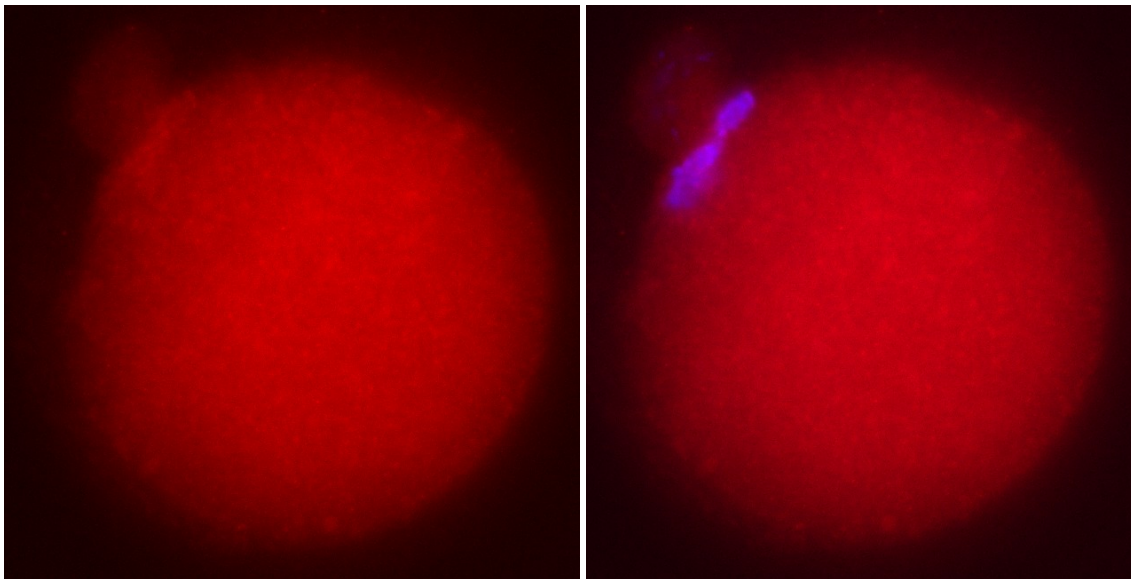


**Figure 31 - The effect of Demecolcine on Rec8 localization in oocytes fixed in Interphase.**

Oocytes were incubated for 10 minutes in 10mM SrCl<sub>2</sub> followed by a 230 minute incubation in media containing both SrCl<sub>2</sub> and 0.4ug/ml Demecolcine. Rec8 alone (*left panel*). Overlay of Rec8 (*red*) and Hoechst 22358 (*blue*) (*right panel*). Rec8 appears to show some localization directly on the chromatin (similar to Figure 30). Red fluorescence is imaged at 150ms.

## Discussion

### ***The effects of Demecolcine on the APC***

Demecolcine has previously been used to assist in the enucleation of mammalian oocytes for nuclear transfer experiments. In order to better understand the efficacy of this process in early development, three key cell cycle regulation proteins (Apc11, Cdc20, and Rec8) were localized in developing mouse embryos in the presence or absence of Demecolcine. It was the working hypothesis of this project that, since these three proteins have been previously described to associate with the meiotic spindle (Harper *et al.*, 2002; Acquaviva *et al.*, 2004; Castro *et al.*, 2005), the disruption of the spindle would affect the localization of these proteins.

As described earlier, the data from the Apc11 localization experiments suggest striking effects of Demecolcine on APC localization. Although Apc11 strongly localized to the perispindular region of the cytoplasm in control oocytes (those incubated in the absence of Demecolcine), in Demecolcine treated eggs, no localization was observed. From these data, one can postulate that without a well organized meiotic spindle, the anaphase promoting complex has nothing around which it will conglomerate. Thus, the localization of Apc11 may be tied directly to the integrity of the meiotic spindle.

Although Cdc20 was not shown to localize to the meiotic spindle in control oocytes, the data from the Cdc20 localization experiments also show pronounced effects of Demecolcine on the APC. In the control activation, Cdc20 localization consistently weakened from punctate cytoplasmic staining at MII to a dim, diffuse pattern after activation. Cdc20 localization continued to diminish through TII only to intensify again at interphase. This cyclic pattern is consistent with previous studies regarding Cdc20's role as both activator and substrate of the anaphase promoting complex (Zacharaie *et al.*, 1999; and many others; see Figure 2). However, in oocytes incubated in Demecolcine, no developmental variation could be detected. Therefore, one could conjecture that Demecolcine has in some way affected the APC's ability to function properly in the orderly binding and destruction of Cdc20.

It is possible that a loss of APC localization caused by the disruption of the spindle could be accompanied by a concomitant loss of APC activity. It has been

hypothesized that the APC ubiquitinates proteins by bringing them into direct contact with the E2 enzyme (Harper, *et al.*, 2002; Kraft *et al.*, 2003; Passmore & Barford, 2004; Castro *et al.*, 2005). In order to do this, it is necessary for the APC to be in direct contact with the substrate. By reducing the concentration of Apc11 around segregation chromosomes (as seen in Figure 15 through Figure 17), an incubation in Demecolcine could limit the ability of the complex to make contact with substrates in that area, thus, preventing ubiquitination of key cell cycle proteins. While this may or may not affect the ubiquitination of securin, which has yet to be localized to the meiotic spindle, it could certainly affect cyclin B, whose destruction inactivates MPF, and other substrates vital to the regulation of the cell cycle known to localize to the perispindular region.

In order to test directly the effects of Demecolcine on APC activity, a series of ubiquitination and deubiquitination assays could be designed. Based on the protocol by Rape *et al.* (2006), the ability of the APC to ubiquitinate APC substrates could be closely examined both in the presence and absence of Demecolcine. Given the effect of Demecolcine on APC localization, one would predict that the ubiquitination of several cell cycle proteins in the vicinity of the meiotic spindle would also be affected while the ubiquitination of those not localized to the spindle would not be severely disturbed. If the results of such experiments did in fact show a disruption or reduction in the ubiquitination of cyclin B (localized to the spindle) but not securin (evenly distributed throughout the cytoplasm), it could provide further evidence that the APC-regulated addition of ubiquitin is indeed a proximity reaction.

The data from the Rec8 localization experiments also indicate a subtle consequence of an incubation in Demecolcine. In control oocytes, Rec8 consistently localized to the region of the cortex directly above chromosomal DNA. However, in Demecolcine treated oocytes, Rec8 appears to amass to the area directly surrounding the chromatin, not in the cortical region above it. Additionally, Rec8 localization appears in a direct colocalization with the chromatin following activation. Since this direct colocalization was not observed in control cells, one can postulate that perhaps the meiotic spindle in some way shields Rec8 from the DNA and the destruction of that spindle frees the chromatin from the protection of the spindle.

With regards to the use of Rec8 as an indirect indicator of APC activity, these results could be interpreted in several ways. Although Rec8 did follow a consistent staining pattern in control eggs, this pattern differed slightly from the localization expected. The main function of Rec8 has been shown in mitotic cells to be the maintenance of the cohesion complex structure at the metaphase plate. The cleavage of Rec8 at the onset of anaphase opens the cohesion ring allowing the proper segregation of sister chromatids (reviewed by Revenkova & Jessberger, 2005). Given this function, one would predict a strong colocalization with cellular chromatin at metaphase which would disappear at the onset of anaphase. Since this direct localization and destruction is not observed, it is possible that Rec8 might serve a different function in the mouse oocyte system and Rec8 would have been a less-than-ideal choice for an indirect indicator of APC activity.

The differences between the predicted and observed Rec8 data are not all that surprising. The prediction was originally based on observations made of Scc1, another member of the kleisin family, in cells undergoing mitosis, not meiosis. At mitotic metaphase, Scc1 localizes directly with the condensed chromatin. At the onset of mitotic anaphase, Scc1 is cleaved by separase, the same enzyme known to be responsible for the excision of Rec8 in meiosis, and disperses throughout the cytoplasm where it is degraded. Because of the similarities between Rec8 and Scc1, one would predict that the two proteins would localize in a similar manner. However, a different localization pattern was observed for Rec8. Perhaps this pattern can be attributed to the inherent differences in the meiotic versus mitotic mechanisms among which are the symmetrical division of the cytoplasmic material, the idiosyncratic gene expression of meiotic cells, and dissolution of SMC complexes in oocytes from arm to centromere (Reviewed by Revenkova & Jessberger, 2005).

### ***Implications for SCNT***

The data presented in the three localization experiments has implications for the field of somatic cell nuclear transfer (SCNT). Recently, Demecolcine has been used to chemically assist the enucleation of oocytes for the purposes of mammalian cloning in several species. While this process has been shown to produce healthy cloned offspring

slightly more efficiently than conventional enucleation methods, the overall efficiency of such procedure remains low. Since the majority of the data presented here indicate that Demecolcine could have a deleterious affect on the localization of the APC, it is conceivable that this could contribute to the low efficiency by reducing the developmental competence of the donor oocytes. Therefore, it would be advantageous to develop a protocol that would continue to exploit the enucleation ability of Demecolcine to assist oocytes in the extrusion of DNA while simultaneously maintaining a high functional activity of the anaphase-promoting complex.

In order to test the effectiveness of such a protocol, ubiquitin assays similar to those described by Rape *et al.* (2006) can be completed on lysates of oocytes enucleated by conventional methods and assisted by Demecolcine. If the APC is shown to be more active in cells enucleated with Demecolcine, this could help to explain the higher efficiency of chemical assisted enucleation.

### ***Future Experiments***

Because the data regarding the effects of Demecolcine (and other MT destabilizing drugs) on the APC are still in their infancy, more experiments that measure APC activity (both directly and indirectly) are required. Firstly, a series of western blots should be designed to measure relative protein concentrations of Cdc20, Rec8, and several other APC substrates like securin and cyclin B at all stages of development. These blots could corroborate the evidence presented earlier that both Cdc20 and Rec8 concentrations normally change significantly as the cell develops. These concentration changes would be closely monitored in the presence and absence of Demecolcine to determine if the drug interferes with the orderly destruction of these and other protein substrates. Since the timely destruction is a hallmark of APC function, these western blots would serve as an indirect measure of APC activity.

Following the Westerns, a sequence of rt-PCR and RNAi experiments could be developed to study gene expression of the anaphase promoting complex and other key cell cycle regulators. Often with conventional SCNT methods, the gene expression of the reconstructed embryo differs from that of the parent organism. This patterning can occur

even if the entire genome is identical. While reasons for this phenomenon have since been attributed to the donor karyoplast, recent experimental observations have suggested that the recipient cytoplasm is equally important in the reprogramming of the gene expression. Thus, it would be invaluable to understand the gene expression of key cell cycle regulators like the Anaphase Promoting Complex following reconstruction into a cytoplasm created by Demecolcine-assisted enucleation.

## Works Cited

Acquaviva, C., Herzog, F., Kraft, C., Pines, J. (2004). "The anaphase promoting complex/cyclosome is recruited to centromeres by the spindle assembly checkpoint". *Nat Cell Biol.* 6(9):892-8.

Allworth, A., Albertini, D. (1993). "Meiotic maturation in cultured bovine oocytes is accompanied by remodeling of the cumulus cell cytoskeleton". *Developmental Biology* 158:101-112.

Baguisi, A., Overstrom, E. (2000). "Induced enucleation in nuclear transfer procedures to produce cloned animals". *Theriogenology* 53: 209.

Bai R, Verdier-Pinard P, Gangwar S, Stessman CC, McClure KJ, Sausville EA, Pettit GR, Bates RB, Hamel E. (2001). "Dolastatin 11, a marine depsipeptide, arrests cells at cytokinesis and induces hyperpolymerization of purified actin." *Mol Pharmacol.* 59(3): 462-9.

Bamburg, J. (1999). "Proteins of the ADF/Cofilin Family: Essential Regulators of Actin Dynamics." *Annu. Rev. Cell Dev. Biol.* 15:185–230.

Brown, S., Spudich, J. (1979). "Cytochalasin inhibits the rate of elongation of actin filament fragments". *J. Cell Biology.* 83: 657-662.

Bubb, M., Senderowicz, *et al.* (1994). "Jasplakinolide, a cytotoxic natural product, induces actin polymerization and competitively inhibits the binding of Phalloidin to F-actin". *J. Biol. Chem.* 269: 14869-14871.

Bubb, M. R., Spector, I., Beyer, B. B. & Fosen, K. M. (2000). "Effects of jasplakinolide on the kinetics of actin polymerization". *J.Biol.Chem.* 275: 5163-5170.

Campbell, K., Alberio, R., Choi, I., Fisher, P., Kelly, R., Lee, J., Maalouf, W. (2005). "Cloning: Eight years after Dolly". *Reprod. Dom. Anim* 40: 256-268.

Carroll, C., Morgan, D. (2002). "The Doc1 subunit is a processivity factor for the anaphase-promoting complex". *Nature Cell Biology* 11: 880-887.

Castro, A., Bernis, C., Vigneron, S., Labbe, JC., Lorca, T. (2005). "The anaphase-promoting complex: a key factor in the regulation of the cell cycle". *Oncogene* 24: 314-325.

Chau, V., Tobias, J. W., Bachmair, A., Marriott, D., Ecker, D.J., Gonda, D. K., and Varshavsky, A. (1989). "A multiubiquitin chain is confined to specific lysine in a targeted short-lived protein". *Science* 243:1576-1583.

- Chen, S.U., Chao, K.H., Chang, C.Y., Hsieh, F.J., Ho, H.N., Yang, Y.S. (2004). "Technical aspects of the piezo, laser-assisted, and conventional methods for nuclear transfer of mouse oocytes and their efficiency and efficacy: Piezo minimizes damage of the ooplasmic membrane at injection". *J Exp Zool A Comp Exp Biol.* 4: 344-51.
- Clute, P., Pines, P. (1999). "Temporal and spatial control of cyclin B1 destruction in metaphase". *Nature Cell Biology* 1: 82-88.
- Cramer, L. (1999). "Role of actin-filament disassembly in lamellipodium protrusion in motile cells revealed using the drug jasplakinolide". *Curr Biol.* 9: 1095-1105.
- Cooper, J., (October 1987). "Effects of Cytochalasin and Phalloidin on Actin" *The Journal of Cell Biology.* Vol 105. 1473-1478.
- Das, A., Cohen, P., Barford, D. (1998). "The structure of the tetratricopeptide repeats of protein phosphatase 5: implications for TPR-mediated protein-protein interactions". *EMBO Journal* 17(5): 1192-1199.
- Furuta, T., Tuck, S., Kirchner, J., Koch, B., Auty, R., Kitagawa, R., Rose, A., Greenstein, D. (2000). "EMB-30: an APC4 homologue required for metaphase-to-anaphase transitions during meiosis and mitosis in *Caenorhabditis elegans*". *Molecular Biology of the Cell* 11: 1401-1419.
- Gmachl, M., Gieffers, C., Podtelejnikov, A., Mann, M., Peters, JM. "The RING-H2 finger protein APC11 and the E2 enzyme UBC4 are sufficient to ubiquitinate substrates of the anaphase-promoting complex". *PNAS* 97(16): 8973-8978.
- Harper, JW., Burton, J., Solomon, M. (2002). "The anaphase promoting complex: it's not just for mitosis any more". *Genes and Development* 16:2179-2206.
- Hartwell, L., Culotti, J., Reid, B. (1970). "Genetic control of the cell-division cycle in yeast. I. Detection of mutants". *Proceedings of the National Academy of Science* 66: 352-359.
- Hayden SM, Miller PS, Brauweiler A, Bamburg. JR. (1993). "Analysis of the interactions of actin depolymerizing factor with G- and F-actin". *Biochemistry* 32:9994-10004.
- Hou, J., Lei, T., Liu, L., Cui, X., An, X., Chen, Y. (2006). "Demecolcine-induced enucleation of sheep meiotically maturing oocytes". *Reprod Nutr Dev.* 46(2):219-26.
- Ibanez, E., Albertini, D., Overstrom, E. (2005). "Effect of genetic background and activating stimulus on the timing of meiotic cell cycle progression in parthenogenetically activated mouse oocytes". *Reproduction* 129: 27-38.
- Ibanez, E., Albertini, D., Overstrom, E. (2003). "Demecolcine-induced oocyte enucleation for somatic cell cloning: coordination between cell-cycle egress, kinetics of

cortical cytoskeletal interactions, and second polar body extrusion". *Biol Reprod.* 68(4): 1249-58.

Jones, K. (2005). "Mammalian egg activation: from Ca<sup>2+</sup> spiking to cell cycle progression". *Reproduction* 130 (6): 813-23.

Jorgensen, P., Brundell, E., Starborg, M., Hoog, C. (1998). "A subunit of the Anaphase-Promoting Complex is a centromere-associated protein in mammalian cells". *Molecular and Cellular Biology*: 468-476.

Jordon, A., Hadfield, J., Lawrence, N., McGown, A., (1998). "Tubulin as a target for anticancer drugs: agents which interact with the mitotic spindle". *Med. Res.* 18(4): 259-296.

Jorgensen, P., Grasland, S., Betz, R., Stahl, S., Larsson C., Hoog, C. (2001). *Gene* 262: 51-59.

Kato, Y., Tetsuya T., Kurokawa, K., Kato, J., Doguchi, H., Yasue, H., Tsunoda, Y., (1998). "Eight calves cloned from somatic cells of a single adult". *Science* 282: 2095-2098.

Kominami K, Seth-Smith H, Toda T. (1998). "Apc10 and Ste9/Srw1, two regulators of the APC-cyclosome, as well as the CDK inhibitor Rum1 are required for G1 cell-cycle arrest in fission yeast". *European Molecular Biology Organization Journal* 17(18): 5388-5399.

Kraft, C., Herzog, F., Gieffers, C., Mechtier, K., Hagting, A., Pines, J., Peters, JM. (2003). "Mitotic regulation of the human anaphase promoting complex by phosphorylation". *EMBO Journal* 22(24): 658-6609.

Lan, G.C., Chang, Z.L., Luo MJ, Jiang, Y.L., Han, D., Wu, Y.G., Han, Z.B., Ma, S.F., Tan, J.H. (2006). "Production of cloned goats by nuclear transfer of cumulus cells and long-term cultured fetal fibroblast cells into abattoir-derived oocytes". *Mol Reprod Dev.* 73(7):834-840.

Lodish, H., Berk, A., Matsudaria, P., Kaiser, C., Krieger, M., Scott, M., Zipursky, L., Darnell, J. *Molecular Cell Biology* 5<sup>th</sup> ed. W H Freeman & Co (Sd) 1999.

Lupas, A., Wolfgang Baumeister, W., Hofmann, K. (1997). A repetitive sequence in subunits of the 26S proteasome and 20S cyclosome (anaphase-promoting complex) *Trends in Biochemical Sciences* 22(6): 195-196.

Ma, S., Kalousek, D., Yuen, B., Moon, Y. (1997). "Investigation of effects of pregnant mare serum gonadotropin (PMSG) on the chromosomal complement of CD-1 mouse embryos". *Journal of Assisted Reproduction and Genetics* 14(3):162-9.

Machaty, Z., Funahashi, H., Mayes, M., Day, B., Prather, R. (1996). "Effects of injecting calcium chloride into in vitro matured porcine oocytes". *Biol Reprod* 54: 316-322.

Mattson, B., Overstrom, E., Albertini, D. (1990). "Transitions in trophectoderm cellular shape and cytoskeletal organization in the elongating pig blastocyst". *Biology of Reproduction* 42:195-200.

McGough, A., Chris J. Staiger, Jung-Ki Min and Karen D. Simonetti (2003). "The gelsolin family of actin regulatory proteins: modular structures, versatile functions". *FEBS*. 552(3): 75-81.

Oda, T., Crane, Z.D., Dicus, C.W., Sufi, B.A., Bates, R.B. (2003). "Dolastatin 11 connects two long-pitch strands in F-actin to stabilize microfilaments". *Journal of Molecular Biology* 328 (2): 319-324.

Passmore LA, Booth CR, Venien-Bryan C, Ludtke SJ, Fioretto C, Johnson LN, Chiu W, Barford D. (2005). "Structural analysis of the anaphase-promoting complex reveals multiple active sites and insights into polyubiquitylation". *Mol Cell*. 20(6):855-66.

Passmore LA and Barford, D. (2004) "Getting into position: the catalytic mechanisms of protein ubiquitylation". *Biochem. J.* 379: 513–525.

Passmore, LA. (2004). "The anaphase-promoting complex: the sum of its parts?". *Biochemical Society Transactions* 32(5): 724-727.

Passmore, L., McCormack, E., Au, S., Paul, A., Willison, K., Harper, J. Barford, D., (2003). "Doc1 mediates the activity of the anaphase-promoting complex by contributing to substrate recognition". *European Molecular Biology Organization Journal* 22(4): 786-796.

Peters, J.M. (2002). "The Anaphase-Promoting Complex: Proteolysis in Mitosis and Beyond". *Molecular Cell* 9: 93-943.

Petroski, M., Deshaies, R. (2005). "Function and Regulation of cullin-RING ubiquitin ligases". *Nature Reviews Molecular Cell Biology* 6, 9-20.

Pines, J., Lindon, C. (2005). "Proteolysis: anytime, any place, anywhere?". *Nat. Cell Biol.* 7: 731-735.

Rabitsch, A. Tóth, M. Gálová, A. Schleiffer, G. Schaffner, E. Aigner, C. Rupp, A. Penkner, A. Moreno-Borchart, M. Primig. (2001). "A screen for genes required for meiosis and spore formation based on whole-genome expression". *Current Biology* 11(13): 1001-1009.

- Ramos, C., Teissie, J. (2000). "Electrofusion: a biophysical modification of cell membrane and a mechanism in exocytosis". *Biochimie*. 82 (5): 511-8.
- Rape, M., Reddy, S., Kirschner, M. (2006). "The Processivity of Multiubiquitination by the APC determines the Order of Substrate Degradation". *Cell* 124: 89-103.
- Revenkova, E., Jessberger, R., (2005). "Keeping sister chromatids together: cohesions in meiosis". *Reproduction* 130(6): 783-790.
- Russell, D., Ibanez, E., Albertini, D., Overstrom, E., (2005). "Activated Bovine Cytoplasts Prepared by Demecolcine-Induced Enucleation Support Development of Nuclear Transfer Embryos In Vitro". *Molecular Reproduction and Development* 72:161-170.
- Salah, S., Nasmyth, K., (2000). "Destruction of the securin Pds1p occurs at the onset of anaphase during both meiotic divisions in yeast". *Chromosoma* 109: 27-34.
- Small, J., Rottner, K., Hahne, P., Anderson, K. (1999). *Microscopy Research and Technique* 47(1): 3-17.
- Smith, L. (2003). "Membrane and intracellular effects of ultraviolet irradiation with Hoechst 33342 on bovine secondary oocytes matured in vitro". *J Reprod Fertil.* 99(1):39-44.
- Takita, M., Furuya, T., Sugita, T., Kawauchi, S., Oga, A., Hirano, T., Tsunoda, S., Sasaki, K. (2003). "An analysis of changes in the expression of cyclins A and B1 by the cell array system during the cell cycle: comparison between cells synchronization methods". *Cytometry Part A* 55A: 24-29.
- Tang, Z., Li, B. Bharadwaj R, Zhu H, Ozkan E, Hakala K, Deisenhofer J, Yu H. (2001). "APC2 Cullin protein and APC11 RING protein comprise the minimal ubiquitin ligase module of the anaphase-promoting complex". *Mol Biol Cell.* 12:3839-51.
- Terret, M., Wassmann, K., Waizenegger, I., Maro, B., Peters, J.M., Verlhac, M.H. (2003). "The meiosis I-to-meiosis II transition in mouse oocytes requires separate activity". *Curr Biol.* 13(20): 1797-1802.
- Tugendreich, S., Tomkiel, J., Earnshaw, W., Hieter, P. (1995). "CDC27Hs colocalizes with CDC16Hs to the centrosome and mitotic spindle and is essential for the metaphase to anaphase transition". *Cell* 81: 261-268.
- Ufano, S., San-Segundo, P., del Rey, F., and Vázquez de Aldana, C. R. (1999). "SWM1, a Developmentally Regulated Gene, Is Required for Spore Wall Assembly in *Saccharomyces cerevisiae*". *Mol. Cell. Biol.* 19: 2118-2129.
- Vajta, G., Lewis, I.M., Hyttel, P., Thouas, G.A., Trounson, A.O. (2001). "Somatic cell cloning without micromanipulators". *Cloning* 3: 89-95.

- Vasquez, R., Howell, B., Yvon, A., Wadsworth, P., Cassimeris, L. (1997). "Nanomolar concentrations of Nocodazole alter microtubule dynamic instability in vivo and in vitro." *Mol Biol Cell* 8(6): 973–985.
- Velilla E, Lopez-Bejar M, Rodriguez-Gonzalez E, Vidal F, Paramio MT., (2002). "Effect of Hoechst 33342 staining on developmental competence of prepubertal goat oocytes". *Zygote* 10(3):201-208.
- Vodermaier, H., Geirffers, C., Maurer-Stroh, S., Eisenhaber, F., Peters, JM. (2003). "TPR Subunits of the Anaphase Promoting Complex Mediate binding to the activator protein Cdh1". *Current Biology* 13:1459-1468.
- Way, M., Pope, B. & Weeds, A. G. (1992). "Evidence for functional homology in the F-actin binding domains of gelsolin and alpha-actinin: implications for the requirements of severing and capping". *J. Cell Biol.* 119: 835-842.
- Wells, D., Misica, P., Day, T., Tervit, H. (1997). "Production of cloned lambs from an established embryonic cell line: a comparison between in vivo- and in vitro- matured cytoplasts". *Biology of Reproduction* 57: 385-393.
- Wilmut I, Schnieke AE, McWhir J, Kind AJ, Campbell KH. (1997). "Viable offspring derived from fetal and adult mammalian cells". *Nature* 385:810-813.
- Wilson, L., Panda D., Jordan, MA. (1999). "Modulation of Microtubule Dynamics by Drugs: a Paradigm for the Actions of Cellular Regulators." *Cell Structure and Function* 24: 329-335.
- Wirth, K., Wutz, G., Kudo, N.R., Desdouets, C., Zetterberg, A., Taghybeeglu, S., Seznec, J., Ducos, G.M., Ricci, R., Firnberg, N., Peters, J.M., Nasmyth, K. (2006). "Separase: a universal trigger for sister chromatid disjunction but not chromosome cycle progression". *Journal of Cellular Biology* 172(6):847-60.
- Zachariae, W., Nasmyth, K. (1999). "Whose end is destruction: cell division and the anaphase-promoting complex". *Genes and Development* 13:2039-2058.
- Zheng N, Schulman BA, Song L, Miller JJ, Jeffrey PD, Wang P, Chu C, Koepp DM, Elledge SJ, Pagano M, Conaway RC, Conaway JW, Harper JW, Pavletich NP. (2002). "Structure of the Cull1-Rbx1-Skp1-F boxSkp2 SCF ubiquitin ligase complex". *Nature* 416(6882):703-9.

## Appendix A: Hela cell split protocol

1. Aspirate media
2. Rinse 3 times with PBS (-Ca<sup>2+</sup>-Mg<sup>2+</sup>)
3. Aspirate PBS
4. Add 1.5 ml trypsin/EDTA
5. When cells have detached from the culture dish, add 5 ml EMEM +FBS and pen/strep
6. Centrifuge at 16,000 rpm for 5 min
7. Aspirate media
8. Resuspend in EMEM

## Appendix B: Chemical Components

### *Media Composition*

#### **FHM**

Base Catalog #	MR-024
Working pH range	7.2 - 7.4
Components	mg/L
CaCl <sub>2</sub> -2H <sub>2</sub> O	251.00
KCL	186.00
KH <sub>2</sub> PO <sub>4</sub>	47.60
MgSO <sub>4</sub> (anhyd.)	24.10
MgSO <sub>4</sub> -7H <sub>2</sub> O	---
NaCl	5550.00
NaHCO <sub>3</sub>	336.00
BSA	1000.00
EDTA	3.80
D-Glucose	36.00
HEPES	4760.00
Hyaluronidase (U/L)	---
Calcium Lactate	---
Sodium Lactate 60% (ml/L)	1.86
Lactate NaSalt (ml/L) 1.42	---
Sodium Pyruvate	22.00

Phenol Red	10.00
L-Glutamine	146.00
Penicillin G Na Salt (u/L)	100,000.00
Streptomycin Sulfate	50.00

<http://www.specialtymedia.com/05Resources/Formulations/mmformulation2.htm>

## KSOM

Base Catalog #	MR-106	MR-107	MR-121
Working pH range	7.2 - 7.4	7.2 - 7.4	7.2 - 7.4
Components	mg/L	mg/L	mg/L
<b>Inorganic Salts</b>			
CaCl <sub>2</sub> ·2H <sub>2</sub> O	250.00	250.00	250.00
KCL	186.38	186.38	186.38
KH <sub>2</sub> PO <sub>4</sub>	47.99	47.99	47.99
MgSO <sub>4</sub>	---	---	0.00
MgSO <sub>4</sub> 7H <sub>2</sub> O	49.30	49.30	49.30
NaCl	5551.80	5551.80	5551.80
NaHCO <sub>3</sub>	2100.25	2100.25	2100.25
<b>Other Components</b>			
EDTA	3.72	3.72	3.72
D-Glucose	36.03	36.03	36.03
Sodium Lactate	1121.00	1121.00	---
Lactate NaSalt (ml/L) 1.42	---	---	1121.00
Sodium Pyruvate	22.00	22.00	22.00
BSA	1000.00	---	1000.00
Phenol Red	----	---	10.00
<b>Amino Acids</b>			
L-Arginine	63.20	63.20	63.20
L-Cystine	12.02	12.02	12.02
L-Cystine-2HCL	---	---	0.00
L-Glutamine	146.15	146.15	146.15
Glycine	3.75	3.75	3.75
L-Histidine	---	---	---
L-Histidine.HCl.H <sub>2</sub> O	20.96	20.96	20.96
L-Isoleucine	26.23	26.23	26.23
L-Leucine	26.24	26.24	26.24
L-Lysine	---	---	---
L-Lysine.HCl	36.52	36.52	36.52
L-Methionine	7.46	7.46	7.46
L-Phenylalanine	16.52	16.52	16.52
L-Serine	5.26	5.26	5.26
L-Threonine	23.82	23.82	23.82
L-Tryptophan	5.11	5.11	5.11

L-Tyrosine	18.12	18.12	18.12
L-Tyrosine NaH <sub>2</sub> O	---	---	0.00
L-Valine	23.42	23.42	23.42
L-Alanine	4.45	4.45	4.45
L-Asparagine	---	---	---
L-Asparagine-H <sub>2</sub> O	7.50	7.50	7.50
L-Aspartic Acid	6.66	6.66	6.66
L-Glutamic Acid	7.36	7.36	7.36
L-Proline	5.76	5.76	5.76
<b>Antibiotics</b>			
Pen G Na Salt (units)	100,000.00	100,000.00	100,000.00
Strep Sulfate	50.00	50.00	50.00

<http://www.specialtymedia.com/05Resources/Formulations/KSOM%20FormulationNew.htm>

### **MTSB-XF**

All chemicals purchased from Sigma Aldrich unless otherwise indicated.

% given in v/v in Phosphate Buffered Saline

PIPES	100mM
MgCl <sub>2</sub>	5mM
EGTA	2.5mM
DTT	1mM
Taxol	1uM
Aprotinin	0.01%
Deuterium oxide	50%
Formaldehyde	3.70%
Triton X-100	0.10%

### **Blocking Buffer**

All chemicals purchased from Sigma Aldrich unless otherwise indicated.

% given in w/v for solid and v/v for liquid chemicals in Phosphate Buffered Saline

Sodium azide	0.20%
Bovine Serum Albumin Fraction V	1%
Powdered milk; Carnation	0.2%
Normal Goat Serum (heat inactivated)	2%
Glycine	0.1M
Triton X-100	0.01%

### ***Blocking Buffer (-goat serum)***

All chemicals purchased from Sigma Aldrich unless otherwise indicated.

% given in w/v for solid and v/v for liquid chemicals in Phosphate Buffered Saline

Sodium azide	0.20%
Bovine Serum Albumin Fraction V	1%
Powdered milk; Carnation	0.2%
Glycine	0.1M
Triton X-100	0.01%